

**THE STUDY OF FLUID FLOWS AND HEAT TRANSFER
NEAR A STAGNATION POINT IN
A NEWTONIAN FLUID**

WONG SIN WEI

**FACULTY OF SCIENCE
UNIVERSITY OF MALAYA
KUALA LUMPUR**

2012

**THE STUDY OF FLUID FLOWS AND HEAT TRANSFER
NEAR A STAGNATION POINT IN
A NEWTONIAN FLUID**

WONG SIN WEI

**DISSERTATION SUBMITTED IN FULFILLMENT OF
THE REQUIREMENTS FOR THE DEGREE OF
MASTER OF SCIENCE**

**INSTITUTE OF MATHEMATICAL SCIENCES
FACULTY OF SCIENCE
UNIVERSITY OF MALAYA
KUALA LUMPUR**

2012

UNIVERSITI MALAYA

ORIGINAL LITERARY WORK DECLARATION

Name of Candidate: WONG SIN WEI

(I.C/Passport No: 870413-56-5034)

Registration/Matric No: SGP 100003

Name of Degree: MASTER OF SCIENCE

Title of Project Paper/Research Report/Dissertation/Thesis ("this Work"):

**THE STUDY OF FLUID FLOWS AND HEAT TRANSFER NEAR A STAGNATION
POINT IN A NEWTONIAN FLUID**

Field of Study: FLUID MECHANICS

I do solemnly and sincerely declare that:

- (1) I am the sole author/writer of this Work;
- (2) This Work is original;
- (3) Any use of any work in which copyright exists was done by way of fair dealing and for permitted purposes and any excerpt or extract from, or reference to or reproduction of any copyright work has been disclosed expressly and sufficiently and the title of the Work and its authorship have been acknowledged in this Work;
- (4) I do not have any actual knowledge nor ought I reasonably to know that the making of this work constitutes an infringement of any copyright work;
- (5) I hereby assign all and every rights in the copyright to this Work to the University of Malaya ("UM"), who henceforth shall be owner of the copyright in this Work and that any reproduction or use in any form or by any means whatsoever is prohibited without the written consent of UM having been first had and obtained;
- (6) I am fully aware that if in the course of making this Work I have infringed any copyright whether intentionally or otherwise, I may be subject to legal action or any other action as may be determined by UM.

Candidate's Signature

Date

Subscribed and solemnly declared before,

Witness's Signature

Date

Name:

Designation:

ABSTRAK

Aliran mantap dua dimensi bendalir likat tak mampat dan pemindahan haba sekitar titik genangan bendalir Newtonan dikaji. Tiga jenis masalah aliran bendalir likat dipertimbangkan. Masalah pertama ialah mengenai kesan daya keapungan ke atas aliran sekitar titik genangan helaian mencancang yang meregang, sementara masalah kedua ialah aliran bendalir likat di atas helaian mendatar yang mengecut atau meregang secara eksponen. Dalam masalah ketiga, kajian terhadap aliran bendalir likat di atas helaian mendatar yang mengecut atau meregang secara eksponen diperluaskan, dengan mengambil kira pelepasan kelikatan dan pemindahan haba. Masalah ini dipengaruhi oleh parameter tertentu, iaitu keapungan, eksponen halaju, sedutan atau suntikan, dan keregangan atau kekecutan sempadan yang bergerak. Daripada tranformasi pembolehubah keserupaan, sistem persamaan pembezaan separa (PPS) dijemakan kepada sistem persamaan pembezaan biasa (PPB). Penyelesaian sistem PPB diselesaikan secara berangka melalui beza terhingga tengah *Keller-box*, yang menurunkan persamaan PPB peringkat ketiga atau yang rendah kepada sistem PPB peringkat satu. Ciri-ciri aliran dan pemindahan haba untuk nilai-nilai parameter yang berbeza dikaji dan dibincangkan. Daripada penyelesaian ini, wujud dua penyelesaian yang bergantung kepada parameter-parameter tertentu di mana selain penyelesaian aliran bendalir yang biasa terdapat pula penyelesaian aliran terbalik.

ABSTRACT

Two-dimensional steady, incompressible viscous fluid flows and heat transfer near a stagnation point in Newtonian fluid are studied. Three different problems of fluid flows are considered. In the first problem buoyancy force on stagnation point flow towards a vertical stretching sheet is studied, whilst the second problem is about viscous fluid flow over an exponentially shrinking or stretching horizontal sheet. In the third problem, the study of viscous fluid flow over an exponentially stretching or shrinking sheet is extended with the inclusion of viscous dissipation and mass transfer. These problems are governed by certain parameters, namely buoyancy, velocity exponents, suction or injection, and stretching or shrinking of the moving boundary. From similarity variables transformations, the governing system of partial differential equations (PDEs) is transformed into a system of ordinary differential equations (ODEs). The solutions of system of ODEs are computed numerically by a central finite difference Keller-box method, which reduces third or lower order ODE to a system of first-order ODEs. The flow features and heat transfer characteristics for different values of the governing parameters are analyzed and discussed. From these solutions, it was found that dual solutions exist at certain range of parameters whereby apart from the normal fluid flow solutions, reverse flow solutions are also obtained.

ACKNOWLEDGEMENTS

First, I would like to express my deepest gratitude to my supervisors, Mr. Md. Abu Omar Awang and Prof. Dr. Anuar Mohd. Ishak, for their guidance, support and patience throughout the years of my post-graduate studies. Their intuition and insight in attacking a problem always fascinated me and their enthusiasm, encouragement and devotion have always been a source of inspiration to me.

A special thanks to my family. I couldn't have reached this point without the invaluable support provided by my family.

I would also like to say thank-you to all those who have supported me in any respect during the life of my research. In fact, I am fortunate to meet those wonderful people who have enriched my life.

Finally, my thanks to Institute of Mathematical Sciences, University of Malaya and also Ministry of Higher Education Malaysia for their financial support for this research.

TABLE OF CONTENTS

ABSTRAK	ii
ABSTRACT	iii
ACKNOWLEDGEMENTS	iv
TABLE OF CONTENTS	v
LIST OF TABLES	viii
LIST OF FIGURES	ix
LIST OF SYMBOLS AND ABBREVIATIONS	xii
CHAPTER 1 INTRODUCTION	
1.1 Background of the Study	1
1.2 Basic Conservation Equation	2
1.2.1 Law of conservation of mass	3
1.2.2 Law of conservation of momentum	5
1.2.3 Law of conservation of energy	9
1.3 Derivation of Boundary Layer Equations	14
1.4 Similarity Transformation	19
1.5 Numerical Implementations	20
1.6 Layout of the Thesis	21

**CHAPTER 2 BUOYANCY FORCE ON STAGNATION-POINT FLOW
TOWARDS A VERTICAL, NON-LINEARLY STRETCHING
SHEET WITH PRESCRIBED SURFACE HEAT FLUX**

2.1	Introduction	23
2.2	Problem Formulation	24
2.3	Results and Discussion	28
2.4	Conclusion	32

**CHAPTER 3 STAGNATION POINT FLOW OVER AN EXPONENTIALLY
SHRINKING/STRETCHING SHEET**

3.1	Introduction	33
3.2	Problem Formulation	35
3.3	Results and Discussion	38
3.4	Conclusion	45

**CHAPTER 4 BOUNDARY LAYER FLOW AND HEAT TRANSFER
OVER AN EXPONENTIALLY STRETCHING/SHRINKING
PERMEABLE SHEET WITH VISCOUS DISSIPATION**

4.1	Introduction	46
4.2	Problem Formulation	48
4.3	Results and Discussion	52
4.3.1	Stretching case, $\varepsilon = 1$	53
4.3.2	Shrinking case, $\varepsilon = -1$	56

4.4	Conclusion	64
CHAPTER 5 CONCLUSIONS AND FUTURE WORK		65
REFERENCES		68

LIST OF TABLES

Tables	Page
4.1 Values of $-\theta'(0)$ for bifurcation points in Figures 4.9 and 4.10	59

LIST OF FIGURES

Figure	Page
1.1 Boundary layer at a flat plate	1
1.2 Stagnation point flow	2
1.3 Fluid particles in box fixed in space	4
1.4 Stresses on a control volume $dx dy dz$ in a fixed frame, only forces in x -direction are shown.	7
2.1 Physical model and coordinate system	24
2.2 Variation of the skin friction coefficient $f''(0)$ with λ for various values of m when $\varepsilon = 0.5$	29
2.3 Variation of the skin friction coefficient $f''(0)$ with λ for various values of m when $\varepsilon = 1$	29
2.4 Variation of the local Nusselt number $1/\theta(0)$ with λ for various values of m when $\varepsilon = 0.5$	31
2.5 Variation of the local Nusselt number $1/\theta(0)$ with λ for various values of m when $\varepsilon = 1$	31
3.1 Physical model and coordinate system	35
3.2 Variation of the skin friction coefficient $f''(0)$ with ε	39
3.3 Variation of the local Nusselt number $-\theta'(0)$ with ε for various values of Pr	40
3.4 Velocity profile $f'(\eta)$ for various values of $\varepsilon < 0$	40
3.5 Temperature profile $\theta(\eta)$ for various values of $\varepsilon < 0$ when Pr = 1	41
3.6 Temperature profile $\theta(\eta)$ for various values of Pr when $\varepsilon = -1.45$	42

3.7	Temperature profile $\theta(\eta)$ for various values of Pr when $\varepsilon = 0.5$	43
3.8	Temperature profile $\theta(\eta)$ for various values of ε when $Pr = 1$	43
3.9	Velocity profile $f'(\eta)$ for various values of ε	44
4.1	Physical model and coordinate system	48
4.2a	Dimensionless stream function $f(\eta)$ for various values of s when $\varepsilon = 1$	52
4.2b	Streamlines for $s = 0$ and $\varepsilon = 1$	52
4.3	Variation of the skin friction coefficient $f''(0)$ with s when $\varepsilon = 1$	53
4.4	Variation of the local Nusselt number $-\theta'(0)$ with s for various values of Pr when $\varepsilon = 1$ and $Ec = 1$	54
4.5	Variation of the local Nusselt number $-\theta'(0)$ with s for various values of Ec when $\varepsilon = 1$ and $Pr = 1$	54
4.6	Velocity profile $f'(\eta)$ for various values of s when $\varepsilon = 1$	55
4.7	Temperature profile $\theta(\eta)$ for various values of s when $\varepsilon = 1$, $Pr = 1$ and $Ec = 1$	56
4.8	Variation of the skin friction coefficient $f''(0)$ with s when $\varepsilon = -1$	57
4.9	Variation of the local Nusselt number $-\theta'(0)$ with s for various values of Pr when $\varepsilon = -1$ and $Ec = 1$	58
4.10	Variation of the local Nusselt number $-\theta'(0)$ with s for various values of Ec when $\varepsilon = -1$ and $Pr = 1$	59
4.11	Temperature $\theta(\eta)$ variation, with $s = 2.3$ and $Ec = 1$, for various values of Pr when $\varepsilon = -1$	60
4.12	Temperature $\theta(\eta)$ variation, with $s = 2.3$ and $Pr = 1$, for various values of	

	Ec when $\varepsilon = -1$	60
4.13	Velocity profile $f'(\eta)$ for various values of s when $\varepsilon = -1$	61
4.14	Temperature profile $\theta(\eta)$ for various values of s when $\varepsilon = -1, \text{Pr} = 1$ and $Ec = 1$	62
4.15	Velocity profile $f'(\eta)$ when $s = 3.5$ for $\varepsilon = \pm 1$	63
4.16	Temperature profile $\theta(\eta)$ for $\varepsilon = \pm 1$ when $s = 3.5, \text{Pr} = 1, Ec = 1$	63

LIST OF SYMBOLS AND ABBREVIATIONS

a, b, c	constants
C_f	skin friction coefficient
C_p	specific heat of the fluid at constant pressure
Ec	Eckert number
f	dimensionless stream function
g	acceleration due to gravity
Gr_x	local Grashof number
k	thermal conductivity
L	reference length
m	velocity exponent parameter
Nu_x	local Nusselt number
Pr	Prandtl number
q_w	surface heat flux
Re_x	local Reynolds number
s	suction/injection parameter
T	fluid temperature
T_∞	ambient temperature
T_w	surface temperature
T_0	constant sheet temperature
U_∞	free stream velocity
U_w	velocity of the shrinking/stretching sheet

u, v	velocity components along the x - and y - directions, respectively
x, y	cartesian coordinates along the surface and normal to it, respectively

Greek Letters

α	thermal diffusivity
β	thermal expansion coefficient
ε	stretching/shrinking parameter
η	similarity variable
θ	dimensionless temperature
λ	buoyancy parameter
μ	dynamic viscosity
ν	kinematic viscosity
ρ	fluid density
τ_w	surface shear stress
ψ	stream function

Subscripts

w	condition at the solid surface
∞	condition far away from the solid surface

Superscript

$'$	differentiation with respect to η
-----	--

CHAPTER 1

INTRODUCTION

1.1 Background of the Study

Fluids, unlike solids, can deform continuously under a shear stress. Our interest in this thesis is to study the flows that are dominated by viscosity and thermal diffusivity, which are known as viscous flows. For a viscous flow over a flat plate, the fluid particles tend to decelerate faster nearer the solid plate surface compared to the free stream, thus creating a thin shear layer called boundary layer. This boundary layer is graphically depicted in Figure 1.1.

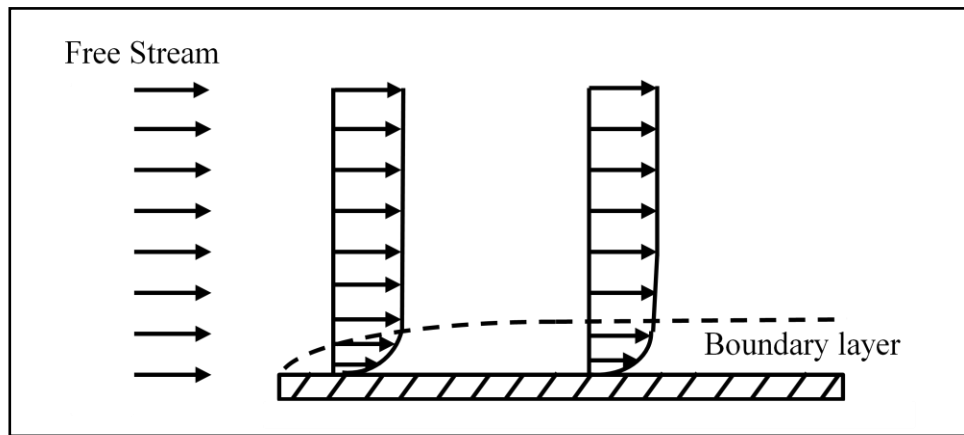


Figure 1.1 Boundary layer at a flat plate

In this study, we are interested in seeing how the viscous action affects the boundary layer thickness, the skin friction (drag force) and the heat transfer rate. We restrict our attention to Newtonian fluid flows near a stagnation point. Here, Newtonian fluids are fluids in which its shear stress is directly proportional to the rate of deformation only. For example water, air and gasoline. Stagnation point is a point in the flow where the

velocity of the fluid is zero, for example as shown in Figure 1.2. The solutions at this stagnation point will give important information on the skin friction and heat transfer rate.

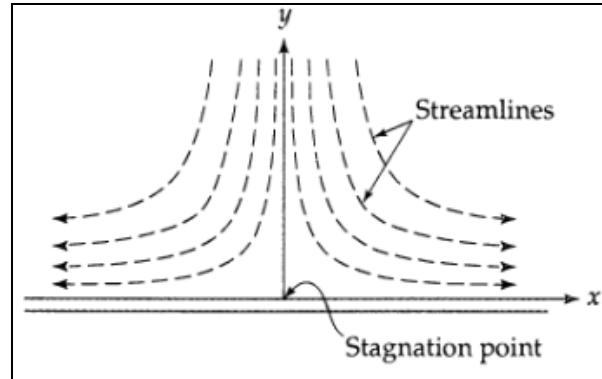


Figure 1.2 Stagnation point flow

In this chapter we develop the fundamental concepts and equations of viscous fluid flow. To begin with, we derive the fundamental equations governing the fluid motion. Then follows the boundary layer equations, whereby the underlying physical and mathematical concepts of boundary layers will be illustrated. Next similarity variables to reduce the system of partial differential equations (PDEs) to system of ordinary differential equations (ODEs) is introduced. Then these ODEs are solved by numerical methods.

1.2 Basic Conservation Equation

The fundamental principles in deriving fluid motion and heat transfer are the laws of conservation of mass, linear and angular momentum and energy. We chose finite control volume method to convert the physical laws to mathematical equations.

1.2.1 Law of conservation of mass

The law of conservation of mass of fluid particles can be derived by considering moving fluid particles entering and leaving a box fixed in space, as shown in Figure 1.3. The velocity components u , v and w of fluid particles are in the direction of x , y and z respectively. The mass flow rate per unit area into the box in the x -direction is given by $\rho u \, dydz$, where ρ is the density of the fluid, whilst the mass flow rate per unit area out of the box in the x -direction is

$$\begin{aligned} & \rho(x+dx)u(x+dx)dydz \\ &= \left(\rho + \frac{\partial \rho}{\partial x} dx + \left(\frac{\partial^2 \rho}{\partial x^2} \right) \frac{(dx)^2}{2!} + \dots \right) \left(u + \frac{\partial u}{\partial x} dx + \left(\frac{\partial^2 u}{\partial x^2} \right) \frac{(dx)^2}{2!} + \dots \right) dydz \\ &= \left[\rho u + \frac{\partial(\rho u)}{\partial x} dx + \text{higher order terms} \right] dydz. \end{aligned}$$

Therefore the net flow rate in the x -direction is $-\frac{\partial}{\partial x}(\rho u) dx dy dz$. The same mass flow rate per unit area are applied in the y -direction and z -direction respectively. Hence, the net flow rate into the box $dx dy dz$ is

$$-\left\{ \frac{\partial}{\partial x}(\rho u) + \frac{\partial}{\partial y}(\rho v) + \frac{\partial}{\partial z}(\rho w) + \text{higher order terms} \right\} dx dy dz. \quad (1.1)$$

The mass increment per unit time of the fluid particles in this fixed box is

$$\frac{\partial}{\partial t}(\rho \, dx \, dy \, dz) = \frac{\partial \rho}{\partial t} \, dx \, dy \, dz. \quad (1.2)$$

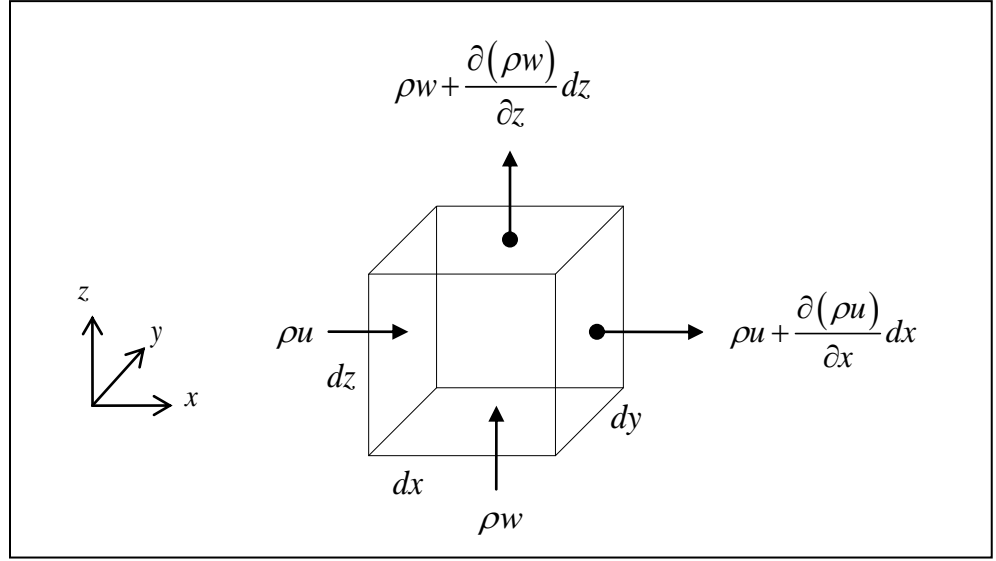


Figure 1.3 Fluid particles in box fixed in space

The laws of conservation of mass states that sum of the rate of mass entering the box fixed in space minus sum of the rate of mass leaving out of the box must equal to the mass increment per unit time in the box fixed in space. Thus combining Equations (1.1) and (1.2) and neglecting higher-order terms yield

$$\frac{\partial \rho}{\partial t} + \frac{\partial}{\partial x}(\rho u) + \frac{\partial}{\partial y}(\rho v) + \frac{\partial}{\partial z}(\rho w) = 0,$$

that is,

$$\frac{D\rho}{Dt} + \rho \nabla \cdot \underline{u} = 0. \quad (1.3)$$

Here $\underline{u} = (u, v, w)$. For incompressible flow $\frac{D\rho}{Dt} = 0$, thus Equation (1.3) reduces to

$$\frac{\partial u}{\partial x} + \frac{\partial v}{\partial y} + \frac{\partial w}{\partial z} = 0. \quad (1.4)$$

Equation (1.4) is normally referred to as Equation of Continuity.

In two-dimensional flow independent of coordinate z , Equation (1.4) becomes

$$\frac{\partial u}{\partial x} + \frac{\partial v}{\partial y} = 0 . \quad (1.5)$$

1.2.2 Law of conservation of momentum

According to the laws of conservation of momentum, which is also called Newton's second law, mass (m) times acceleration (a) is equal to sum of the applied forces. In viscous flow, there are two types of forces to be considered, which are body forces (pressure) and surface forces (friction forces). The body forces act on every fluid particle of the body whereas the surface forces acts on the fluid surface element only, and these create the deformation of the fluid. If \underline{f}_b is the body force per unit volume, \underline{f}_s the surface force per unit area, and \underline{F} is the sum of all body and surface forces, the relationship for the momentum equation in a control volume $dx dy dz$ is

$$\underline{F} = m \underline{a} ; \quad \underline{F} = \underline{f}_b + \underline{f}_s . \quad (1.6)$$

Recall that the mass of the fluid particles in a control volume $dx dy dz$ in a fixed frame of reference is

$$m = \rho \, dx \, dy \, dz , \quad (1.7)$$

and the acceleration of the fluid particles in Cartesian coordinate is

$$\begin{aligned} \underline{a} &= \frac{D \underline{u}}{Dt} \\ &= \frac{\partial \underline{u}}{\partial t} + \underline{u} \cdot \nabla \underline{u} \end{aligned} \quad (1.8)$$

where D/Dt is the material derivative, $\partial \underline{u}/\partial t$ is local acceleration and $\underline{u} \cdot \nabla \underline{u}$ is the convective acceleration. Therefore, the acceleration field in x , y and z direction respectively will be

$$\begin{aligned}\frac{Du}{Dt} &= \frac{\partial u}{\partial t} + u \frac{\partial u}{\partial x} + v \frac{\partial u}{\partial y} + w \frac{\partial u}{\partial z} , \\ \frac{Dv}{Dt} &= \frac{\partial v}{\partial t} + u \frac{\partial v}{\partial x} + v \frac{\partial v}{\partial y} + w \frac{\partial v}{\partial z} , \\ \frac{Dw}{Dt} &= \frac{\partial w}{\partial t} + u \frac{\partial w}{\partial x} + v \frac{\partial w}{\partial y} + w \frac{\partial w}{\partial z} .\end{aligned}\tag{1.9}$$

In order to determine the surface forces, consider the diagram shown in Figure 1.4. Stresses are defined as surface forces per unit surface area. Normal stresses σ are stress components that act perpendicularly to surface of control volume $dx dy dz$, while tangential (shear) stresses τ are the components in the plane of the surface of control volume $dx dy dz$. The surface forces can be expressed as follows:

$$\begin{aligned}\text{in the } x - \text{direction: } &\left(\frac{\partial \sigma_{xx}}{\partial x} + \frac{\partial \tau_{xy}}{\partial y} + \frac{\partial \tau_{xz}}{\partial z} \right) dx dy dz , \\ \text{in the } y - \text{direction: } &\left(\frac{\partial \tau_{yx}}{\partial x} + \frac{\partial \sigma_{yy}}{\partial y} + \frac{\partial \tau_{yz}}{\partial z} \right) dx dy dz , \\ \text{in the } z - \text{direction: } &\left(\frac{\partial \tau_{zx}}{\partial x} + \frac{\partial \tau_{zy}}{\partial y} + \frac{\partial \sigma_{zz}}{\partial z} \right) dx dy dz .\end{aligned}\tag{1.10}$$

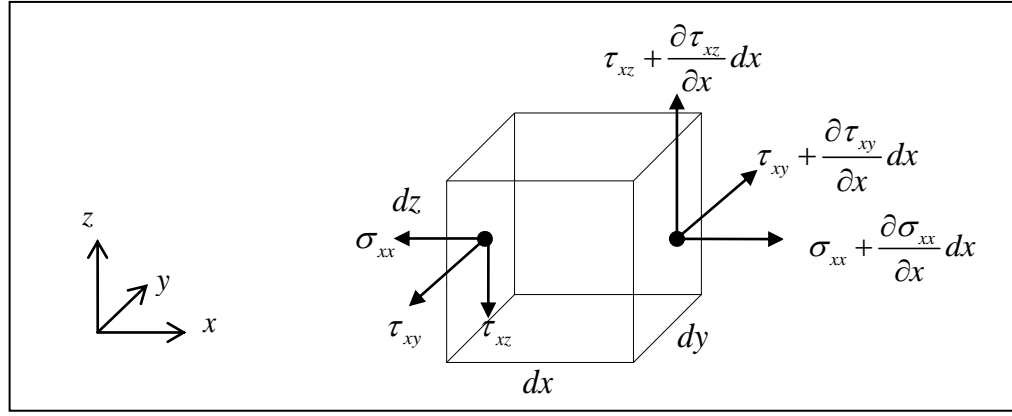


Figure 1.4 Stresses on a control volume $dx dy dz$ in a fixed frame, only forces in x –direction are shown.

Let body force per unit volume be $\rho \tilde{f}_b$, with $\tilde{f}_b = \langle f_x, f_y, f_z \rangle$. Substituting Equation (1.7), (1.9), (1.10) into (1.6), the momentum equations become

$$\begin{aligned} \rho \frac{Du}{Dt} &= \rho f_x + \frac{\partial \sigma_{xx}}{\partial x} + \frac{\partial \tau_{xy}}{\partial y} + \frac{\partial \tau_{xz}}{\partial z}, \\ \rho \frac{Dv}{Dt} &= \rho f_y + \frac{\partial \tau_{yx}}{\partial x} + \frac{\partial \sigma_{yy}}{\partial y} + \frac{\partial \tau_{yz}}{\partial z}, \\ \rho \frac{Dw}{Dt} &= \rho f_z + \frac{\partial \tau_{zx}}{\partial x} + \frac{\partial \tau_{zy}}{\partial y} + \frac{\partial \sigma_{zz}}{\partial z}, \end{aligned} \quad (1.11)$$

where the volume $dx dy dz$ of the fluid particles in control volume has been eliminated. Equation (1.11) is called Navier-Stokes Equations. To solve for u , v and w , we have to obtain suitable expression for the stresses in terms of the velocity and pressure field. Using the Stokes Hypothesis (conservation of angular momentum) as suggested by Stokes in 1849 (detailed derivations may be found in Daily and Harleman (1966), Schlichting (1979), and White (2000)), the stresses can be expressed as follows:

$$\tau_{xy} = \mu \left(\frac{\partial v}{\partial x} + \frac{\partial u}{\partial y} \right),$$

$$\tau_{yz} = \mu \left(\frac{\partial w}{\partial y} + \frac{\partial v}{\partial z} \right),$$

$$\tau_{zx} = \mu \left(\frac{\partial u}{\partial z} + \frac{\partial w}{\partial x} \right), \quad (1.12)$$

$$\sigma_{xx} = -p - \frac{2}{3} \mu \nabla \cdot \underline{u} + 2\mu \frac{\partial u}{\partial x},$$

$$\sigma_{yy} = -p - \frac{2}{3} \mu \nabla \cdot \underline{u} + 2\mu \frac{\partial v}{\partial y},$$

$$\sigma_{zz} = -p - \frac{2}{3} \mu \nabla \cdot \underline{u} + 2\mu \frac{\partial w}{\partial z},$$

where μ is viscosity of the fluid, ∇ is gradient operator and $(\nabla \cdot \underline{u}) = \frac{\partial u}{\partial x} + \frac{\partial v}{\partial y} + \frac{\partial w}{\partial z}$. p is

the local thermodynamic pressure, defined as $p = -(\sigma_{xx} + \sigma_{yy} + \sigma_{zz})/3$. Substituting

Equation (1.12) into (1.11), we obtain

$$\rho \frac{Du}{Dt} = \rho f_x - \frac{\partial p}{\partial x} + \frac{\partial}{\partial x} \left[\mu \left(2 \frac{\partial u}{\partial x} - \frac{2}{3} \nabla \cdot \underline{u} \right) \right] + \frac{\partial}{\partial y} \left[\mu \left(\frac{\partial u}{\partial y} + \frac{\partial v}{\partial x} \right) \right] + \frac{\partial}{\partial z} \left[\mu \left(\frac{\partial w}{\partial x} + \frac{\partial u}{\partial z} \right) \right],$$

$$\rho \frac{Dv}{Dt} = \rho f_y - \frac{\partial p}{\partial y} + \frac{\partial}{\partial y} \left[\mu \left(2 \frac{\partial v}{\partial y} - \frac{2}{3} \nabla \cdot \underline{u} \right) \right] + \frac{\partial}{\partial x} \left[\mu \left(\frac{\partial u}{\partial y} + \frac{\partial v}{\partial x} \right) \right] + \frac{\partial}{\partial z} \left[\mu \left(\frac{\partial v}{\partial z} + \frac{\partial w}{\partial y} \right) \right], \quad (1.13)$$

$$\rho \frac{Dw}{Dt} = \rho f_z - \frac{\partial p}{\partial z} + \frac{\partial}{\partial z} \left[\mu \left(2 \frac{\partial w}{\partial z} - \frac{2}{3} \nabla \cdot \underline{u} \right) \right] + \frac{\partial}{\partial x} \left[\mu \left(\frac{\partial w}{\partial x} + \frac{\partial u}{\partial z} \right) \right] + \frac{\partial}{\partial y} \left[\mu \left(\frac{\partial w}{\partial z} + \frac{\partial w}{\partial y} \right) \right].$$

These equations are the complete Navier-Stokes equations for three-dimensional, unsteady, and compressible viscous flow in Cartesian coordinates.

If viscosity μ is constant and $(\nabla \cdot \underline{u})$ is zero i.e the fluid is incompressible, Equation (1.13)

is significantly reduced to

$$\begin{aligned}\rho \left(\frac{\partial u}{\partial t} + u \frac{\partial u}{\partial x} + v \frac{\partial u}{\partial y} + w \frac{\partial u}{\partial z} \right) &= -\frac{\partial p}{\partial x} + \mu \left(\frac{\partial^2 u}{\partial x^2} + \frac{\partial^2 u}{\partial y^2} + \frac{\partial^2 u}{\partial z^2} \right) + \rho f_x, \\ \rho \left(\frac{\partial v}{\partial t} + u \frac{\partial v}{\partial x} + v \frac{\partial v}{\partial y} + w \frac{\partial v}{\partial z} \right) &= -\frac{\partial p}{\partial y} + \mu \left(\frac{\partial^2 v}{\partial x^2} + \frac{\partial^2 v}{\partial y^2} + \frac{\partial^2 v}{\partial z^2} \right) + \rho f_y, \\ \rho \left(\frac{\partial w}{\partial t} + u \frac{\partial w}{\partial x} + v \frac{\partial w}{\partial y} + w \frac{\partial w}{\partial z} \right) &= -\frac{\partial p}{\partial z} + \mu \left(\frac{\partial^2 w}{\partial x^2} + \frac{\partial^2 w}{\partial y^2} + \frac{\partial^2 w}{\partial z^2} \right) + \rho f_z, \\ \rho \frac{Du}{Dt} &= -\nabla p + \mu \nabla^2 \underline{u} + \rho \underline{f}_b.\end{aligned}\tag{1.14}$$

For steady, two-dimensional compressible flow Equation (1.14) becomes

$$\rho \left(u \frac{\partial u}{\partial x} + v \frac{\partial u}{\partial y} \right) = -\frac{\partial p}{\partial x} + \mu \left(\frac{\partial^2 u}{\partial x^2} + \frac{\partial^2 u}{\partial y^2} \right) + \rho f_x,\tag{1.15}$$

$$\rho \left(u \frac{\partial v}{\partial x} + v \frac{\partial v}{\partial y} \right) = -\frac{\partial p}{\partial y} + \mu \left(\frac{\partial^2 v}{\partial x^2} + \frac{\partial^2 v}{\partial y^2} \right) + \rho f_y.\tag{1.16}$$

1.2.3 Law of conservation of energy

The equation for the conservation of energy can be deduced using the same approach as used when deriving the momentum equations. The first law of thermodynamics states that sum of the heat supplied and the work done on the fluid particles in a control volume $dx dy dz$ is equal to the total energy gained in unit time, that is

$$\frac{DE}{Dt} = Q + W, \quad (1.17)$$

where E is the total energy, Q is the heat supplied and W is the work done on the fluid. Let heat flux vector $\underline{q} = \langle q_x, q_y, q_z \rangle$ denotes the heat transferred per unit surface area. The heat entering the box fixed in space in the x -direction is $q_x dy dz$ and the heat transferred out of the box is $[q_x + (\partial q_x / \partial x) dx] dy dz$. Therefore, the net total heat flux transferred in x -direction is $Q_x = -(\partial q_x / \partial x) dx dy dz$. The same applies in the y and z direction. Thus, the total heat supply is

$$\begin{aligned} Q &= - \left(\frac{\partial q_x}{\partial x} + \frac{\partial q_y}{\partial y} + \frac{\partial q_z}{\partial z} \right) dx dy dz \\ &= -(\nabla \cdot \underline{q}) dV, \end{aligned} \quad (1.18)$$

where $dV = dx dy dz$. Assuming small temperature differences, from Fourier (1822) heat law, the heat conduction for the fluid is

$$q_x = -k \frac{\partial T}{\partial x}, \quad q_y = -k \frac{\partial T}{\partial y}, \quad q_z = -k \frac{\partial T}{\partial z},$$

that is, $\underline{q} = -k \nabla T,$ (1.19)

where the thermal conductivity k is a positive physical property. Thus, Equation (1.18) becomes

$$\begin{aligned} Q &= - \left(\frac{\partial}{\partial x} \left(-k \frac{\partial T}{\partial x} \right) + \frac{\partial}{\partial y} \left(-k \frac{\partial T}{\partial y} \right) + \frac{\partial}{\partial z} \left(-k \frac{\partial T}{\partial z} \right) \right) dx dy dz \\ &= \nabla \cdot (k \nabla T) dV \end{aligned} \quad (1.20)$$

Next, we derived the work done W on the fluid. Work done W on a moving fluid particle in a fixed box is equal to the product of its velocity and the component of the stress forces in the direction of velocity. Hence work done on moving fluid particles by the stress forces in the x direction is simply the velocity in the x direction u multiply by the stress forces. With the aid of Figure (1.4), work done by the stress forces on the surface $dydz$ of control volume $dx dy dz$ in the x direction is

$$\begin{aligned}
 u(x+dx)\sigma_{xx}(x+dx)dydz &= \left[u\sigma_{xx} + \frac{\partial(u\sigma_{xx})}{\partial x} dx + \text{higher order term} \right] dydz \\
 u(y+dy)\tau_{xy}(y+dy)dx dz &= \left[u\tau_{xy} + \frac{\partial(u\tau_{xy})}{\partial y} dy + \text{higher order term} \right] dx dz \\
 u(z+dz)\tau_{xz}(z+dz)dx dy &= \left[u\tau_{xz} + \frac{\partial(u\tau_{xz})}{\partial z} dz + \text{higher order term} \right] dx dy
 \end{aligned} \tag{1.21}$$

Neglecting the higher order terms, the net work done by the stress forces acting in the x direction is

$$\begin{aligned}
 & \left[\left(u\tau_{xx} + \frac{\partial(u\sigma_{xx})}{\partial x} dx \right) - u\tau_{xx} \right] dydz + \left[\left(u\tau_{xy} + \frac{\partial(u\tau_{xy})}{\partial y} dy \right) - u\tau_{xy} \right] dx dz \\
 & + \left[\left(u\tau_{xz} + \frac{\partial(u\tau_{xz})}{\partial z} dz \right) - u\tau_{xz} \right] dx dy \\
 & = \left[\frac{\partial(u\sigma_{xx})}{\partial x} + \frac{\partial(u\tau_{xy})}{\partial y} + \frac{\partial(u\tau_{xz})}{\partial z} \right] dx dy dz
 \end{aligned} \tag{1.22}$$

The net work done by stress forces in the y and z directions can be obtained in a similar manner, that is

$$\text{in the } y - \text{direction: } \left(\frac{\partial(v\tau_{xy})}{\partial x} + \frac{\partial(v\sigma_{yy})}{\partial y} + \frac{\partial(v\tau_{yz})}{\partial z} \right) dx dy dz , \quad (1.23)$$

$$\text{in the } z - \text{direction: } \left(\frac{\partial(w\tau_{xz})}{\partial x} + \frac{\partial(w\tau_{zy})}{\partial y} + \frac{\partial(w\sigma_{zz})}{\partial z} \right) dx dy dz .$$

Combining and rearranging these results, the total work done in control volume $dx dy dz$ is

$$W = \left[\frac{\partial}{\partial x} (u\sigma_{xx} + v\tau_{xy} + w\tau_{xz}) + \frac{\partial}{\partial y} (v\sigma_{yy} + u\tau_{yx} + w\tau_{yz}) + \frac{\partial}{\partial z} (w\sigma_{zz} + u\tau_{zx} + v\tau_{zy}) \right] dx dy dz . \quad (1.24)$$

Using Stokes' Hypothesis (1.12) into the work done, we obtained

$$\begin{aligned} & \frac{\partial}{\partial x} (u\sigma_{xx} + v\tau_{xy} + w\tau_{xz}) + \frac{\partial}{\partial y} (v\sigma_{yy} + u\tau_{yx} + w\tau_{yz}) + \frac{\partial}{\partial z} (w\sigma_{zz} + u\tau_{zx} + v\tau_{zy}) \\ &= \frac{\partial}{\partial x} \left\{ u \left[2\mu \frac{\partial u}{\partial x} - \frac{2}{3} \mu \left(\frac{\partial u}{\partial x} + \frac{\partial v}{\partial y} + \frac{\partial w}{\partial z} \right) \right] + v \left[\mu \left(\frac{\partial v}{\partial x} + \frac{\partial u}{\partial y} \right) \right] + w \left[\mu \left(\frac{\partial w}{\partial x} + \frac{\partial u}{\partial z} \right) \right] \right\} \\ &+ \frac{\partial}{\partial y} \left\{ v \left[2\mu \frac{\partial v}{\partial y} - \frac{2}{3} \mu \left(\frac{\partial u}{\partial x} + \frac{\partial v}{\partial y} + \frac{\partial w}{\partial z} \right) \right] + u \left[\mu \left(\frac{\partial u}{\partial y} + \frac{\partial v}{\partial x} \right) \right] + w \left[\mu \left(\frac{\partial w}{\partial y} + \frac{\partial v}{\partial z} \right) \right] \right\} \\ &+ \frac{\partial}{\partial z} \left\{ w \left[2\mu \frac{\partial w}{\partial z} - \frac{2}{3} \mu \left(\frac{\partial u}{\partial x} + \frac{\partial v}{\partial y} + \frac{\partial w}{\partial z} \right) \right] + u \left[\mu \left(\frac{\partial u}{\partial z} + \frac{\partial w}{\partial x} \right) \right] + v \left[\mu \left(\frac{\partial v}{\partial z} + \frac{\partial w}{\partial y} \right) \right] \right\} \end{aligned} \quad (1.25)$$

Finally, the total energy E per unit time is the sum of the internal energy (ρe) and kinetic energy ($\frac{1}{2} \rho |\underline{u}|^2$). This is given by

$$\frac{DE}{Dt} = \frac{D(\rho e + \frac{1}{2} \rho |\underline{u}|^2)}{Dt} dx dy dz . \quad (1.26)$$

Substituting Equation (1.20), (1.24) and (1.25) into (1.17), we obtain the general form of the energy equation.

However, from thermodynamics, the energy equation can also be expressed in terms of enthalpy h by

$$h = e + \frac{P}{\rho}. \quad (1.27)$$

By using the general relation as suggested by Kestin (1966),

$$\frac{Dh}{Dt} = c_p \frac{DT}{Dt} + \frac{1 - \beta T}{\rho} \frac{Dp}{Dt}, \quad (1.28)$$

where c_p is the specify heat capacity at constant pressure and $\beta = -\frac{1}{\rho} \left(\frac{\partial \rho}{\partial T} \right)_p$ is the

coefficient of thermal expansion, the energy equation can thus be rewritten as

$$c_p \frac{DT}{Dt} = \left(\frac{\partial}{\partial x} \left(k \frac{\partial T}{\partial x} \right) + \frac{\partial}{\partial y} \left(k \frac{\partial T}{\partial y} \right) + \frac{\partial}{\partial z} \left(k \frac{\partial T}{\partial z} \right) \right) + \beta T \frac{Dp}{Dt} + \phi, \quad (1.29)$$

where ϕ is the viscous dissipation function, defined as

$$\begin{aligned} \frac{\phi}{\mu} = & 2 \left[\left(\frac{\partial u}{\partial x} \right)^2 + \left(\frac{\partial v}{\partial y} \right)^2 + \left(\frac{\partial w}{\partial z} \right)^2 \right] + \left(\frac{\partial v}{\partial x} + \frac{\partial u}{\partial y} \right)^2 + \left(\frac{\partial w}{\partial y} + \frac{\partial v}{\partial z} \right)^2 \\ & + \left(\frac{\partial u}{\partial z} + \frac{\partial w}{\partial x} \right)^2 - \frac{2}{3} \left(\frac{\partial u}{\partial x} + \frac{\partial v}{\partial y} + \frac{\partial w}{\partial z} \right)^2. \end{aligned} \quad (1.30)$$

If there is no energy dissipation, then the viscous dissipation term can be ignored, and for steady, two-dimensional incompressible flow, Equation (1.29) reduces to

$$u \frac{\partial T}{\partial x} + v \frac{\partial T}{\partial y} = \alpha \frac{\partial^2 T}{\partial x^2} + \alpha \frac{\partial^2 T}{\partial y^2}, \quad (1.31)$$

where $\alpha = k / \rho c_p$.

1.3 Derivation of Boundary Layer Equations

Now consider the general equations of motion (1.3), (1.14), and energy (1.29). In our study, we are going to restrict the analysis to steady, laminar two-dimensional and incompressible fluid flows. Then the fluid flows and heat equations reduce to

$$\frac{\partial u}{\partial x} + \frac{\partial v}{\partial y} = 0, \quad (1.5)$$

$$u \frac{\partial u}{\partial x} + v \frac{\partial u}{\partial y} = -\frac{1}{\rho} \frac{\partial p}{\partial x} + \nu \left(\frac{\partial^2 u}{\partial x^2} + \frac{\partial^2 u}{\partial y^2} \right) + f_x, \quad (1.32)$$

$$u \frac{\partial v}{\partial x} + v \frac{\partial v}{\partial y} = -\frac{1}{\rho} \frac{\partial p}{\partial y} + \nu \left(\frac{\partial^2 v}{\partial x^2} + \frac{\partial^2 v}{\partial y^2} \right) + f_y, \quad (1.33)$$

$$u \frac{\partial T}{\partial x} + v \frac{\partial T}{\partial y} = \alpha \frac{\partial^2 T}{\partial x^2} + \alpha \frac{\partial^2 T}{\partial y^2}. \quad (1.31)$$

Then we apply the boundary layer concept introduced by Ludwig Prandtl in 1904. He proposed that there is a thin region of viscous flow which is confined very close to the solid boundary (such that the no slip boundary condition is obeyed), outside which the flow is inviscid. Since the boundary layer is comparatively very thin, we start by examining the relative sizes of each term in these equations using the order of magnitude

argument. As a typical illustration, consider the flow past a horizontal plate. Let the x -axis lie along the horizontal plane and y -axis perpendicular to it. Let δ be the thickness of the boundary layer where $\delta \ll 1$, l is the length of the plate and also is $O(1)$, and u is the velocity that varies from 0 at the solid surface to U_∞ of the main stream. Therefore

$$x = O(l), \quad y = O(\delta), \quad u = O(U_\infty). \quad (1.34)$$

From the continuity equation (1.5), their order of magnitudes is;

$$\begin{aligned} \frac{\partial u}{\partial x} + \frac{\partial v}{\partial y} &= 0, \\ O\left(\frac{U_\infty}{l}\right), O\left(\frac{v}{\delta}\right). \end{aligned} \quad (1.35)$$

Since both terms in the equation are of the same order of magnitude, the magnitude of velocity v is $O(U_\infty \delta / l)$.

Now, examine the order of magnitude of Equation (1.32), and relegating the body force f_x to later consideration, we see that

$$u \frac{\partial u}{\partial x} + v \frac{\partial u}{\partial y} = -\frac{1}{\rho} \frac{\partial p}{\partial x} + \nu \left(\frac{\partial^2 u}{\partial x^2} + \frac{\partial^2 u}{\partial y^2} \right),$$

gives
$$O\left(U_\infty \frac{U_\infty}{l}\right), O\left(\frac{U_\infty \delta U_\infty}{l \delta}\right) = O\left(\frac{1}{\rho} \frac{\rho U_\infty^2}{l}\right), O\left(\nu \frac{U_\infty}{l^2}\right), O\left(\nu \frac{U_\infty}{\delta^2}\right).$$

Multiplying by $\frac{l}{U_\infty^2}$, this becomes

$$O(1), O(1) = O(1), O\left(\frac{\nu}{U_\infty l}\right), O\left(\frac{\nu}{U_\infty l} \left(\frac{l}{\delta}\right)^2\right) \quad (1.36)$$

Now the term $\partial^2 u / \partial x^2$ can be neglected when compared with the term $\partial^2 u / \partial y^2$, because

$$\frac{\partial^2 u}{\partial x^2} \bigg/ \frac{\partial^2 u}{\partial y^2} = O\left(\frac{\delta}{l}\right)^2 \ll 1. \quad (1.37)$$

Since the diffusion term $\nu(\partial^2 u / \partial y^2)$ must have an order of magnitude of $O(1)$, we see that

$$\delta \approx O\left(\frac{\nu l}{U_\infty}\right)^{1/2} = O\left(l \text{Re}^{-1/2}\right) \ll 1, \quad (1.38)$$

where Reynolds number $\text{Re} = \frac{U_\infty l}{\nu} \gg 1$. Hence, Equation (1.32) now becomes

$$u \frac{\partial u}{\partial x} + \nu \frac{\partial u}{\partial y} = -\frac{1}{\rho} \frac{\partial p}{\partial x} + \nu \frac{\partial^2 u}{\partial y^2}, \quad (1.39)$$

in the limit $R \rightarrow \infty$.

Similarly, postponing the discussion on body force f_y , the order of magnitude for Equation (1.33) is;

$$\begin{aligned} u \frac{\partial v}{\partial x} + \nu \frac{\partial v}{\partial y} &= -\frac{1}{\rho} \frac{\partial p}{\partial y} + \nu \left(\frac{\partial^2 v}{\partial x^2} + \frac{\partial^2 v}{\partial y^2} \right), \\ O\left(U_\infty \frac{U_\infty \delta}{l^2}\right), O\left(\left(\frac{U_\infty \delta}{l}\right)^2 \frac{1}{\delta}\right) &= O\left(\frac{1}{\rho} \frac{\rho U_\infty^2}{\delta}\right), O\left(\nu \frac{U_\infty \delta}{l^2}\right), O\left(\nu \frac{U_\infty \delta}{\delta^2 l}\right) \end{aligned}$$

Multiply by $\frac{\delta}{U_\infty^2}$,

$$O\left(\frac{\delta^2}{l^2}\right), O\left(\frac{\delta^2}{l^2}\right) = O(1), O\left(\frac{\nu\delta^2}{U_\infty l^2}\right), O\left(\frac{\nu}{U_\infty l}\right) \quad (1.40)$$

From the Equation (1.40), we see that only the terms $-\frac{1}{\rho} \frac{\partial p}{\partial y}$ has $O(1)$ whilst the rest tends to 0 as $\delta \rightarrow 0$ (or $R \rightarrow \infty$). Therefore, we are left with

$$-\frac{1}{\rho} \frac{\partial p}{\partial y} = 0. \quad (1.41)$$

The equation $\partial p / \partial y = 0$ is important; it implies that the pressure is constant across the boundary layer. Hence the pressure p is only varying in the x -direction, that is $p = p(x)$.

The same argument can be used for energy equation (1.31), yielding

$$u \frac{\partial T}{\partial x} + v \frac{\partial T}{\partial y} = \alpha \frac{\partial^2 T}{\partial y^2} \quad (1.42)$$

For comprehensive derivation of the boundary layer equations, please refer to the books of Schlichting (1979) and Acheson (1990).

The system of differential equations (1.39), (1.41) and (1.42) must be supplemented by a set of appropriate boundary conditions. For example, the appropriate boundary conditions for the above flat plate flow and heat transfer can be given by

$$u = U(x), \quad v = 0, \quad T = T_w \quad \text{when } y = 0, \quad 0 \leq x \leq l, \quad (1.43)$$

$$u = U_\infty, \quad v = 0, \quad T \rightarrow T_\infty \quad \text{at } y \rightarrow \infty, \quad 0 \leq x \leq l. \quad (1.44)$$

Now we can relate the pressure to the free stream velocity as follows. Using the boundary conditions at $y \rightarrow \infty$ and substituting Equations (1.44) into (1.39), we have

$$U_{\infty} \frac{dU_{\infty}}{dx} = -\frac{1}{\rho} \frac{\partial p}{\partial x} \quad (1.45)$$

Then, replacing the pressure field of (1.45) into (1.39), we obtain

$$u \frac{\partial u}{\partial x} + v \frac{\partial u}{\partial y} = U_{\infty} \frac{dU_{\infty}}{dx} + \nu \frac{\partial^2 u}{\partial y^2}. \quad (1.46)$$

Under these simplifying assumptions, the appropriate equations for the boundary layer are:

$$\frac{\partial u}{\partial x} + \frac{\partial v}{\partial y} = 0, \quad (1.5)$$

$$u \frac{\partial u}{\partial x} + v \frac{\partial u}{\partial y} = U_{\infty} \frac{dU_{\infty}}{dx} + \nu \frac{\partial^2 u}{\partial y^2}, \quad (1.46)$$

$$u \frac{\partial T}{\partial x} + v \frac{\partial T}{\partial y} = \alpha \frac{\partial^2 T}{\partial y^2}, \quad (1.42)$$

with boundary conditions

$$u = u_w, \quad v = 0, \quad T = T(x) \quad \text{when} \quad y = 0, \quad 0 \leq x \leq l, \quad (1.47)$$

$$u \rightarrow U_{\infty}, \quad T \rightarrow T_{\infty} \quad \text{as} \quad y \rightarrow \infty, \quad 0 \leq x \leq l.$$

The solution of Equations (1.5), (1.42) and (1.46) subject to the boundary conditions (1.47) yields the velocity and temperature profiles of the boundary layer. However, our other

main objective of this study is to compute the local skin friction (C_f) and the local Nusselt number (Nu_x) which is related to heat transfer rate at the surface. These are given by

$$C_f = \frac{\tau_w}{\rho U_\infty^2 / 2}, \quad (1.48)$$

and

$$Nu_x = \frac{xq_w}{k(T_w - T_\infty)}, \quad (1.49)$$

where the surface shear stress τ_w and the temperature gradient at the wall q_w are given by

$$\tau_w = \mu \left(\frac{\partial u}{\partial y} \right)_{y=0} \quad \text{and} \quad q_w = -k \left(\frac{\partial T}{\partial y} \right)_{y=0}, \quad (1.50)$$

where w denote the values of τ and q at the wall.

1.4 Similarity Transformation

In this thesis a similarity transformation is used to simplify the system of equation (1.5), (1.42), and (1.46) subject to the boundary conditions (1.47). We use the similarity variables introduced by the previous researchers (see Magyari & Keller 1999; Ishak 2009) to reduce the number of independent variables from two to one. By using these similarity variables, the system of partial differential equations (1.46) and (1.42) will be reduced to nonlinear ordinary differential equation. Similar ideas also apply to the boundary conditions in (1.47). The specific similarity variables will be discussed in each of the following chapters, depending on the problem.

1.5 Numerical Implementations

In this research, we have used an efficient and accurate finite difference scheme, Keller-box method, to solve the system of nonlinear ODEs subject to the appropriate boundary conditions. This method was first suggested by Keller (1970). Its implementation is described in Keller and Cebeci (1971, 1972). An interesting feature of this method is that it is unconditionally stable and is second order accurate. Several authors for instance Ishak et al. (2007, 2009a), Ali et al. (2011), Saha et al. (2007) and Yih (1998) have successfully used this method to solve various fluid flow and heat transfer problems.

The basic idea of the Keller-box method is:

- (i) First, introduce new dependent variables and reduce the system of nonlinear ODE to a first-order system of ODEs.
- (ii) Replace the derivatives of the first order system of ODEs by central differences.
- (iii) Linearize the resulting algebraic equations by Newton's method, and write them in matrix-vector form.
- (iv) The linearized difference equations are solved by the block tridiagonal elimination technique (Thomas method).

In our calculations, we have used step size $\Delta\eta = 0.001$ with a convergence criterion of error less than 10^{-6} . The location of the edge of the boundary layer η_∞ has been adjusted appropriately for different values of parameters to maintain the necessary accuracy. For all the problems discussed, MATLAB has been used for coding.

1.6 Layout of the Thesis

In Chapter 2, 3, and 4 we are going to discuss specific boundary layer problems. The relevant conclusions will be presented at the end of each chapter. These are part of published and unpublished results.

In Chapter 2, we consider the two-dimensional stagnation point flow past a vertical sheet. The sheet is stretched non-linearly; with the velocity and prescribed surface heat flux in power law form. We give a lot of consideration to the effect of buoyancy force and velocity ratio toward the boundary layer problems. Both assisting and opposing buoyant flows are considered. Our results show that assisting buoyant flow has unique solution whilst an increase in velocity ratio leads to an increase in the solution range.

In Chapter 3 the two-dimensional stagnation-point flow due to shrinking or stretching sheet is studied. Here, the shrinking or stretching velocity, the free stream velocity and the surface temperature are in an exponential form, which is different from those in Chapter 2. We investigate the existence and (non)uniqueness of solutions, for both shrinking and stretching sheet. Our results indicate that the solutions in shrinking sheet are not unique.

In Chapter 4, we extend the problem of Chapter 3 by the inclusion of mass transfer and viscous forces. Therefore in this chapter we discuss the two-dimensional stagnation-point flow over an exponentially stretching or shrinking permeable sheet with the additional effects of viscous forces and mass transfer. Our numerical results show that in shrinking boundary layer with wall injection no solution will exist.

In our last chapter, Chapter 5, we present the summary of our research. The conclusions, suggestions or recommendations are discussed in this chapter.

CHAPTER 2

BUOYANCY FORCE ON STAGNATION-POINT FLOW TOWARDS A VERTICAL, NON-LINEARLY STRETCHING SHEET WITH PRESCRIBED SURFACE HEAT FLUX

2.1 Introduction

The study of stagnation point fluid flow and heat transfer due to a nonlinearly stretching surface has significant application in the industrial processes. For example hot metal plate in a cooling bath, production of metal or polymer sheet and manufacturing of glass fiber. The quality of the final product greatly depends on the heat transfer at the stretching surface as explained by Karwe and Jaluria (1988, 1991).

Our objective is to discuss the flow and heat transfer characteristics that are brought about by buoyancy force towards a vertical stretching sheet. Several works that have been reported in this type of flow field (Gupta & Gupta 1977; Nazar et al. 2004; Chen 1998). Ramachandran et al. (1988) studied the effect of buoyancy force on the stagnation point flows past a vertically heated surface at rest and found that dual solutions exist in the buoyancy opposing flow region. Ishak et al. (2008a) extended the idea of Ramachandran (1988) to the fluid induced by the velocity ratio parameter. Ishak et al. (2009a) also considered unsteady flow along stretching sheet and showed that unsteadiness parameter increases the solution range. Moreover, Ishak et al. (2008b, 2008c) have numerically studied the flow induced by stretching vertical sheet in micropolar fluid and MHD fluid.

Motivated by the above investigations, in this research we study the stagnation-point flow towards a nonlinearly stretching sheet with prescribed surface heat flux. The stretching velocity, the free stream velocity and the surface heat flux are assumed to vary in the power-law form.

2.2 Problem Formulation

Consider a mixed convection stagnation-point flow towards a vertical nonlinearly stretching sheet immersed in an incompressible viscous fluid, as shown in Figure 2.1. The Cartesian coordinates (x, y) are taken such that the x -axis is measured along the sheet oriented in the upwards or downwards direction and the y -axis is normal to it.

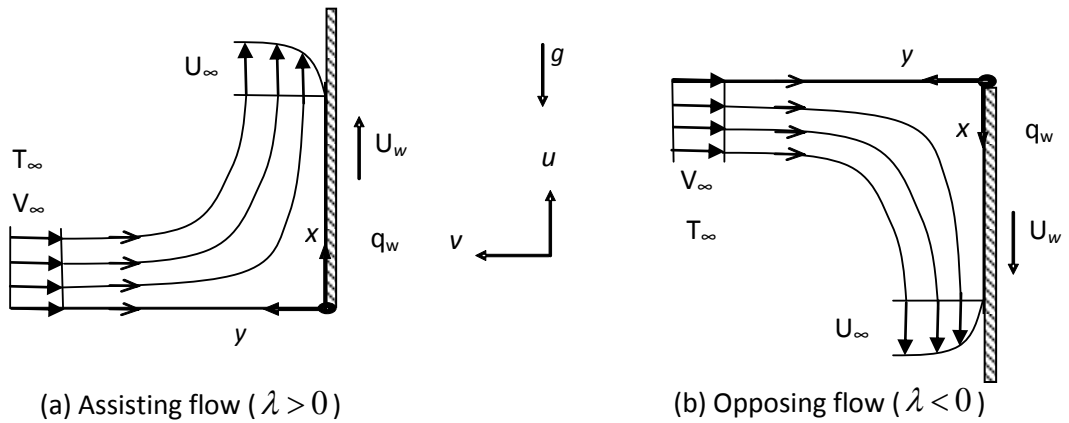


Figure 2.1 Physical model and coordinate system

It is assumed that the wall stretching velocity is given by $U_w = ax^m$ and the far field inviscid velocity distribution in the neighborhood of the stagnation point $(0,0)$ is given by $U_\infty(x) = bx^m$, $V_\infty(y) = -by^m$. The surface heat flux is in the form of $q_w(x) = cx^{(5m-3)/2}$ (see Merkin & Mahmood, 1989), where a , b , c , and m are constants. This $q_w(x)$ ensured

the buoyancy parameter is independent of x . For assisting flow, in Figure 2.1(a) the x –axis points upwards in the same direction of the stretching surface such that the external flow and the stretching surface will induce flow and heat transfer in the velocity and thermal boundary layers respectively. On the other hand, for opposing flow in Figure 2.1(b), the x –axis points vertically downwards in the same direction of the stretching surface such that the external flow and the stretching surface will also induce flow and heat transfer respectively in the velocity and thermal boundary layers. The steady boundary layer equations, with Boussinesq approximation, are

$$\frac{\partial u}{\partial x} + \frac{\partial v}{\partial y} = 0, \quad (2.1)$$

$$u \frac{\partial u}{\partial x} + v \frac{\partial u}{\partial y} = U_{\infty} \frac{dU_{\infty}}{dx} + \nu \frac{\partial^2 u}{\partial y^2} + g \beta (T - T_{\infty}), \quad (2.2)$$

$$u \frac{\partial T}{\partial x} + v \frac{\partial T}{\partial y} = \alpha \frac{\partial^2 T}{\partial y^2}, \quad (2.3)$$

subject to the boundary conditions

$$\begin{aligned} u &= U_w(x), \quad v = 0, \quad \frac{\partial T}{\partial y} = -\frac{q_w}{k} \quad \text{at } y = 0, \\ u &\rightarrow U_{\infty}(x), \quad T \rightarrow T_{\infty} \quad \text{as } y \rightarrow \infty, \end{aligned} \quad (2.4)$$

where u and v are the velocity components along the x – and y – axes, respectively, g is the acceleration due to gravity, α is the thermal diffusivity of the fluid, ν is the

kinematic viscosity, β is the coefficient of thermal expansion and ρ is the fluid density.

T_∞ is the far field ambient constant temperature.

The continuity equation (2.1) can be satisfied automatically by introducing a stream function ψ such that $u = \partial\psi/\partial y$ and $v = -\partial\psi/\partial x$. The momentum and energy equations are transformed by the similarity variables

$$\eta = \left(\frac{U_\infty}{\nu x}\right)^{1/2} y, \quad \psi = [\nu x U_\infty]^{1/2} f(\eta), \quad \theta(\eta) = \frac{k(T - T_\infty)}{q_w} \left(\frac{U_\infty}{\nu x}\right)^{1/2} \quad (2.5)$$

into the following nonlinear ordinary differential equations:

$$f''' + \frac{m+1}{2} ff'' + m(1 - f'^2) + \lambda\theta = 0, \quad (2.6)$$

$$\frac{1}{\text{Pr}}\theta'' + \frac{m+1}{2} f\theta' - (2m-1)f'\theta = 0. \quad (2.7)$$

Here primes denote differentiation with respect to η , $\lambda = Gr_x / \text{Re}_x^{5/2}$ is the buoyancy or mixed convection parameter, $\text{Pr} = \nu/\alpha$ is the Prandtl number, $Gr_x = g\beta q_w x^4 / (k\nu^2)$ is the local Grashof number and $\text{Re}_x = U_\infty x / \nu$ is the local Reynolds number. We note that λ is a constant, with $\lambda > 0$ corresponds to assisting flow and $\lambda < 0$ denote opposing flow whilst $\lambda = 0$ is for forced convective flow.

The transformed boundary conditions are

$$\begin{aligned} f(0) &= 0, & f'(0) &= \varepsilon, & \theta'(0) &= -1, \\ f'(\eta) &\rightarrow 1, & \theta(\eta) &\rightarrow 0 \text{ as } \eta \rightarrow \infty, \end{aligned} \quad (2.8)$$

where $\varepsilon = a/b$.

The physical quantities of interest are the skin friction coefficient C_f and the local Nusselt number Nu_x , which are defined as

$$C_f = \frac{\tau_w}{\rho U_\infty^2 / 2}, \quad Nu_x = \frac{x q_w}{k(T_w - T_\infty)} \quad (2.9)$$

respectively, where the surface shear stress τ_w and the surface heat flux q_w are given by

$$\tau_w = \mu \left(\frac{\partial u}{\partial y} \right)_{y=0}, \quad q_w = -k \left(\frac{\partial T}{\partial y} \right)_{y=0} \quad (2.10)$$

with μ and k being the dynamic viscosity and thermal conductivity, respectively. Using the non-dimensional variables (2.5), we obtain

$$\frac{1}{2} C_f \text{Re}_x^{1/2} = f''(0), \quad \frac{Nu_x}{\text{Re}_x^{1/2}} = \frac{1}{\theta(0)}. \quad (2.11)$$

2.3 Results and Discussion

Equations (2.6) and (2.7) subject to the boundary conditions (2.8) are integrated numerically using a finite difference scheme known as the Keller box method (Keller 1970). Numerical results are presented for different physical parameters. To conserve space, we consider Prandtl number unity throughout this paper. The results presented here, whenever it is comparable, agree very well with those of Ramachandran et al. (1988).

Figures 2.2 and 2.3 show the skin friction coefficient $f''(0)$ against buoyancy parameter λ for some values of velocity exponent parameter m for velocity ratio parameter $\varepsilon = 0.5$ and $\varepsilon = 1$. Two branches of solutions are found. The solid lines are the upper branch solutions and the dash lines are the lower branch solutions. With increasing m , the dual solutions' range increases. Also from both figures of the upper branch solutions, the skin friction is higher for assisting buoyancy flow ($\lambda > 0$) compared to the opposing flow ($\lambda < 0$). This implies that increasing buoyancy convection parameter λ increases the skin friction coefficient $f''(0)$. Whilst for $\varepsilon = 1$ the values of $f''(0)$ in Figure 2.3 are positive for $\lambda > 0$ and negative for $\lambda < 0$. Physically, this means positive $f''(0)$ implies the fluid exerts a drag force on the sheet and negative implies the reverse. Similarly this also happens for $\varepsilon = 0.5$ but at different values of λ .

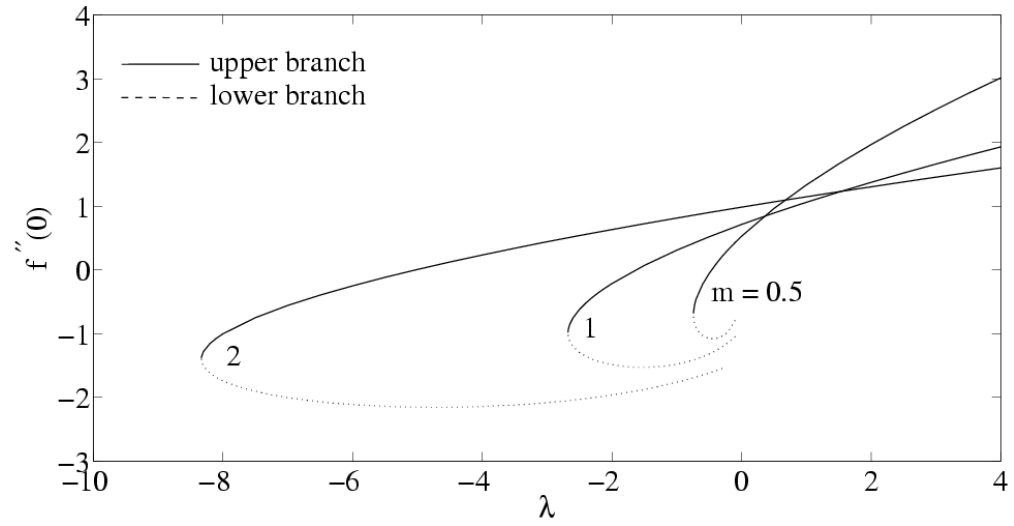


Figure 2.2 Variation of the skin friction coefficient $f''(0)$ with λ for various values of m when $\varepsilon = 0.5$

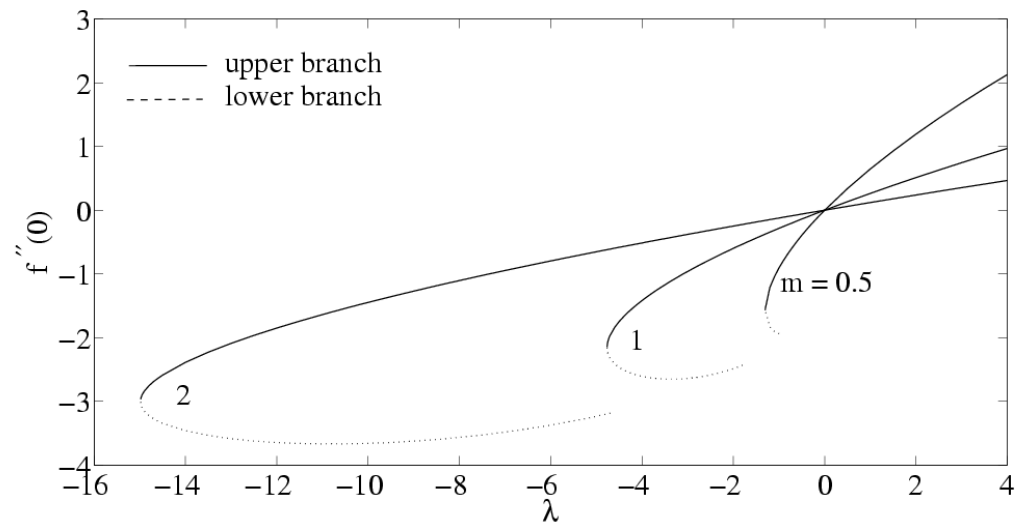


Figure 2.3 Variation of the skin friction coefficient $f''(0)$ with λ for various values of m when $\varepsilon = 1$

As seen in Figures 2.2 and 2.3, there exist a critical value of buoyancy λ_c such that for $\lambda < \lambda_c$ there will be no solutions, for $\lambda_c < \lambda < 0$ there will be dual solutions, and when $\lambda > 0$ the solution is unique. Our numerical calculations in Figure 2.2 shows that for velocity ratio $\varepsilon = 0.5$ $\lambda_c = -8.331, -2.677$ and -0.7411 for $m = 2, 1$ and 0.5 respectively, while in Figure 2.3 for velocity ratio $\varepsilon = 1$, $\lambda_c = -14.98, -4.764$ and -1.301 for $m = 2, 1$ and 0.5 respectively. The dual solutions exhibit the normal forward flow behavior and also the reverse flow where $f'(\eta) < 0$. From these two results, it seems that an increase in velocity ratio parameter ε leads to an increase of the critical values of $|\lambda_c|$. This increases the dual solutions range of Equations (2.6)-(2.8).

Figures 2.4 and 2.5 display the variations of the local Nusselt number $1/\theta(0)$ against buoyant parameter λ , for some values of m when velocity ratio $\varepsilon = 0.5$ and $\varepsilon = 1$ respectively. Both figures clearly show that the local Nusselt number increases as m increases for the upper branch solutions. For the lower branch solutions, the local Nusselt number becomes unbounded as $\lambda \rightarrow 0^-$. Positive values of $1/\theta(0)$ denote that heat is being transferred from the sheet to the fluid, and vice versa.

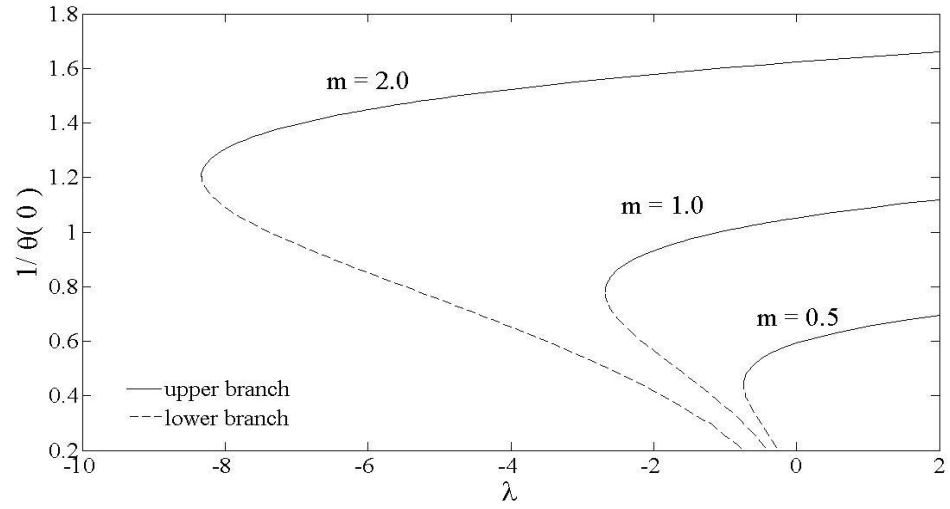


Figure 2.4 Variation of the local Nusselt number $1/\theta(0)$ with λ for various values of m when $\varepsilon = 0.5$

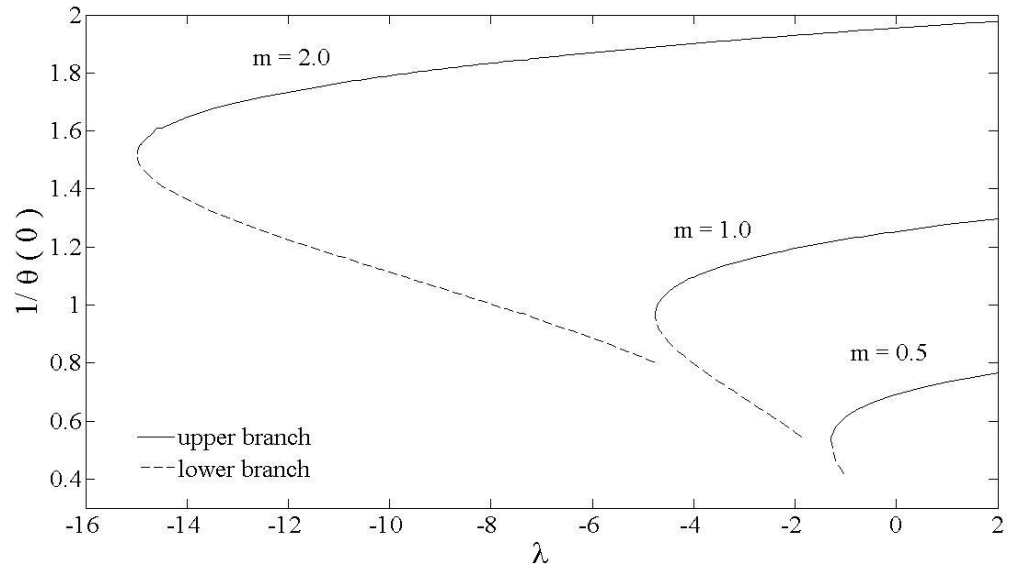


Figure 2.5 Variation of the local Nusselt number $1/\theta(0)$ with λ for various values of m when $\varepsilon = 1$

2.4 Conclusions

The problem of mixed convective stagnation-point flow towards a nonlinearly stretching vertical sheet immersed in an incompressible viscous fluid was investigated numerically. The effects of the governing parameters m , λ and ε on the fluid flow and heat transfer characteristics were discussed. It was found that for assisting flow, the solution is unique, while dual solutions were found to exist for opposing flow up to a certain critical value λ_c . Moreover increasing the velocity exponent parameter m , the solution range of Equations (2.6) –(2.8) increases.

CHAPTER 3

STAGNATION-POINT FLOW OVER AN EXPONENTIALLY SHRINKING/STRETCHING SHEET

3.1 Introduction

Started from early of the last century, there have been numerous sophisticated studies on boundary layer flow. The effects of viscosity and thermal conductivity are important in this layer. Thus, this leads to an urge to understand the underlying physical, mathematical and modeling concepts inherent in boundary layer. In reality, a majority of the applications for the industrial manufacturing processes have to deal with fluid flow and heat transfer behaviors. Examples include the polymer sheet extrusion from a dye, gaseous diffusion, heat pipes, drawing of plastic film and etc. Such processes play an important role to determine the quality of the final products as described by Karwe and Jaluria (1988, 1991).

Crane (1970) was the first person who initiated the study of two-dimensional steady flow of an incompressible viscous fluid induced by a linearly stretching plate. The boundary layer equations were simplified using a similarity transformation, which transformed the governing partial differential equations to a single ordinary differential equation. Since then, there were similar flows that have been considered by several researchers (Andersson et al. 1992; Gupta & Gupta 1977; Nazar et al. 2004; Hossain & Takhar 1996; Ishak et al. 2006a). Such similar flows have been studied extensively in various forms, for example flows with suction/injection, stretching, MHD effect, radiation or non-Newtonian fluids. Magyari and Keller (1999) reported the similarity solutions

describing the steady plane (flow and thermal) boundary layers on an exponentially stretching continuous surface with an exponential temperature distribution. This problem was then extended by Bidin and Nazar (2009), Sajid and Hayat (2008) and Nadeem et al. (2010a, 2010b) to include the effect of thermal radiation, while Pal (2010) and Ishak (2011) studied the similar problem but in the presence of magnetic field. Sanjayanand and Khan (2006) studied the heat and mass transfer in a viscoelastic boundary layer flow over an exponentially stretching sheet. The mixed convection flow of a micropolar fluid over an exponentially stretching sheet was considered by El-Aziz (2009). The problems in non-Newtonian fluids considered in Sanjayanand and Khan (2006) and El-Aziz (2009) do not admit similarity solutions, and thus the authors reported local similarity solutions with certain assumptions.

Recently, the shrinking aspect has become a brand new topic. The abnormal behavior in the fluid flow due to a shrinking sheet has gained attention from several researchers. However, the work on it is relatively little. The flow induced by a shrinking sheet was first discussed by Miklavčič and Wang (2006), where the existence and (non)uniqueness of solutions in both numerical and exact solutions were proven. Extension to that, Fang (2008) carried out the shrinking problem to power law surface velocity with mass transfer. It was shown that the solution only exist with mass suction for the rapidly shrinking sheet problem. Furthermore, Wang (2008) has investigated that the shrinking sheet problem has many unique characteristics. Later on, Sajid et al. (2008) studied the MHD rotating flow over a shrinking surface. It was found that the results in the case of hydrodynamic flow are not stable for the shrinking surface and only meaningful in the presence of magnetic field. The flow over a shrinking sheet in a porous medium was studied by Nadeem and Awais (2008). On the other hand, Ishak et al. (2010a) solved

numerically micropolar fluid flow over a linearly shrinking sheet, and found that the solutions are not unique in shrinking sheet. Very recently, Nadeem et al. (2009, 2010a, 2010b) studied the stagnation point flow over a shrinking sheet in non-Newtonian fluids.

Motivated by the above investigations, here we study the steady two dimensional stagnation point flow over an exponentially shrinking/stretching sheet. The shrinking/stretching velocity, the free stream velocity and the surface temperature are assumed to vary in an exponential form with the distance from the stagnation point. The skin friction coefficient and the local Nusselt number are determined for the understanding of the flow and heat transfer characteristics. The practical applications include the cooling of extruded materials in industrial processes using an inward directed fan or conical liquid jets.

3.2 Problem Formulation

Consider a stagnation-point flow over an exponentially shrinking/stretching sheet immersed in an incompressible viscous fluid as shown in Figure 3.1. The Cartesian coordinates (x, y) are taken such that the x -axis is measured along the sheet, while the y -axis is normal to it.

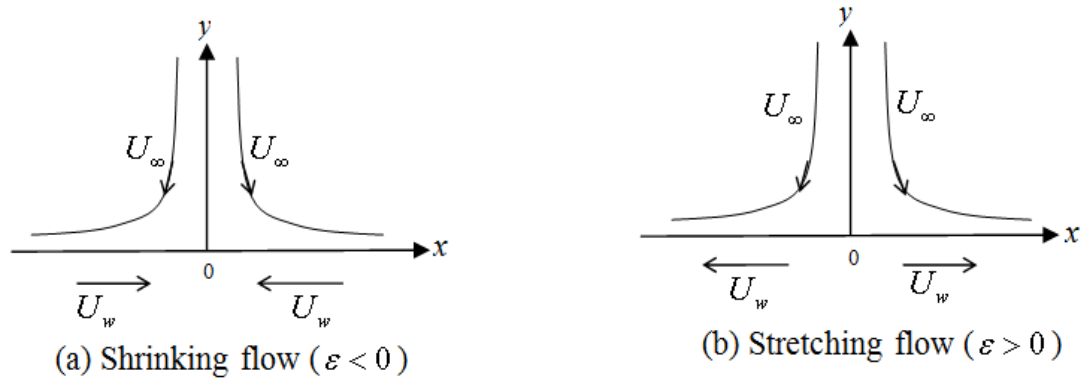


Figure 3.1 Physical model and coordinate system

It is assumed that the free stream velocity, the shrinking/stretching velocity and the surface temperature are given by $U_\infty = ae^{x/L}$, $U_w = be^{x/L}$ and $T_w = T_\infty + ce^{x/L}$, respectively, where a , b and c are constants and L is the reference length. The boundary layer equations are (Magyari and Keller 1999; Ishak et al. 2009b; Bhattacharya & Layek 2011)

$$\frac{\partial u}{\partial x} + \frac{\partial v}{\partial y} = 0, \quad (3.1)$$

$$u \frac{\partial u}{\partial x} + v \frac{\partial u}{\partial y} = U_\infty \frac{dU_\infty}{dx} + \nu \frac{\partial^2 u}{\partial y^2}, \quad (3.2)$$

$$u \frac{\partial T}{\partial x} + v \frac{\partial T}{\partial y} = \alpha \frac{\partial^2 T}{\partial y^2}, \quad (3.3)$$

subject to the boundary conditions

$$u = U_w, \quad v = 0, \quad T = T_w \quad \text{at } y = 0,$$

$$u \rightarrow U_\infty, \quad T \rightarrow T_\infty \quad \text{as } y \rightarrow \infty, \quad (3.4)$$

where u and v are the velocity components along the x – and y – axes, respectively, α is the thermal diffusivity of the fluid and ν is the kinematic viscosity.

Introducing the following similarity transformation (see Magyari & Keller 1999),

$$\eta = \left(\frac{a}{2\nu L} \right)^{1/2} e^{x/(2L)} y, \quad u = ae^{x/L} f'(\eta), \quad v = - \left(\frac{\nu a}{2L} \right)^{1/2} e^{x/(2L)} (f + \eta f'),$$

$$\theta(\eta) = \frac{T - T_\infty}{T_w - T_\infty}, \quad (3.5)$$

the continuity equation (3.1) is automatically satisfied, and Equations (3.2) and (3.3) are reduced to

$$f''' + ff'' - 2f'^2 + 2 = 0, \quad (3.6)$$

$$\frac{1}{\text{Pr}} \theta'' + f\theta' - 2f'\theta = 0, \quad (3.7)$$

where primes denote differentiation with respect to η and $\text{Pr} = \nu/\alpha$ is the Prandtl number.

The transformed boundary conditions are

$$\begin{aligned} f(0) &= 0, \quad f'(0) = \varepsilon, \quad \theta(0) = 1, \\ f'(\eta) &\rightarrow 1, \quad \theta(\eta) \rightarrow 0 \text{ as } \eta \rightarrow \infty, \end{aligned} \quad (3.8)$$

with $\varepsilon = b/a$ being the shrinking/stretching parameter. We note that $\varepsilon < 0$ is for shrinking, $\varepsilon > 0$ for stretching and $\varepsilon = 0$ corresponds to a fixed sheet.

The main physical quantities of interest are the skin friction coefficient and the local Nusselt number, which are proportional to the quantities $f''(0)$ and $-\theta'(0)$, respectively. Thus, our aim is to investigate how the values of $f''(0)$ and $-\theta'(0)$ vary with the shrinking or stretching parameter ε and the Prandtl number Pr .

3.3 Results and Discussion

Graphical results are presented for different physical parameters appearing in the present model. We note that Equations (3.6) and (3.7) are decoupled, and thus the flow field is not affected by the thermal field.

Figure 3.2 shows the variations of the skin friction coefficient $f''(0)$ against shrinking/ stretching parameter ε , while the respective local Nusselt number $-\theta'(0)$ are presented in Figure 3.3. Two branches of solutions are found to exist within the range $\varepsilon_c < \varepsilon \leq -1$, while for $\varepsilon > -1$, the solution is unique. It is seen that for negative values of ε (shrinking case), there is a critical value ε_c where the upper branch meets the lower branch. Based on our computation, $\varepsilon_c \cong -1.4872$. Beyond this critical value, no solution exists. In these figures, the solid lines denote the upper branch, while the dash lines denote the lower branch solutions. It is also evident from these figures that, the range of ε for which the solution exists is very small for the shrinking case. This is due to the vorticity that almost cannot be confined in the boundary layer. It is observed in Figure 3.3 that the lower branch solutions show discontinuity at $\varepsilon \cong -1.145$, -1.255 and -1.375 for $Pr = 0.72$, 1.0 and 1.5 respectively. This phenomenon has been observed by other researchers in the literature, for different problems, for example Ridha (1996) and Ishak et al. (2008d, 2010b). Further, it is found that when $\varepsilon = 1$ (stretching case), the value of the skin friction coefficient $f''(0)$ is zero. This is because when $\varepsilon = 1$, the stretching velocity is equal to the external velocity, and thus there is no friction between the fluid and the solid surface. Furthermore, when $\varepsilon = 1$, the exact solution of Equation (3.6) subject to the boundary condition (3.8) can be obtained, and is given by $f(\eta) = \eta$, which then implies $f''(\eta) = 0$

for all η . The present numerical result agreed with this exact solution. It is also observed that for the upper branch solution, $f''(0) > 0$ when $\varepsilon < 1$ and $f''(0) < 0$ when $\varepsilon > 1$. Physically, positive value of $f''(0)$ means the fluid exerts a drag force on the sheet, and negative value means the opposite. On the other hand, the negative value of $f''(0)$ for the lower branch solution as shown in Figure 3.2 is due to the back flow, see Figure 3.4. The velocity gradient at the surface is negative for $\varepsilon = -1$ and $\varepsilon = -1.2$, but is positive for $\varepsilon = -1.45$, which is in agreement with the results presented in Figure 3.2.

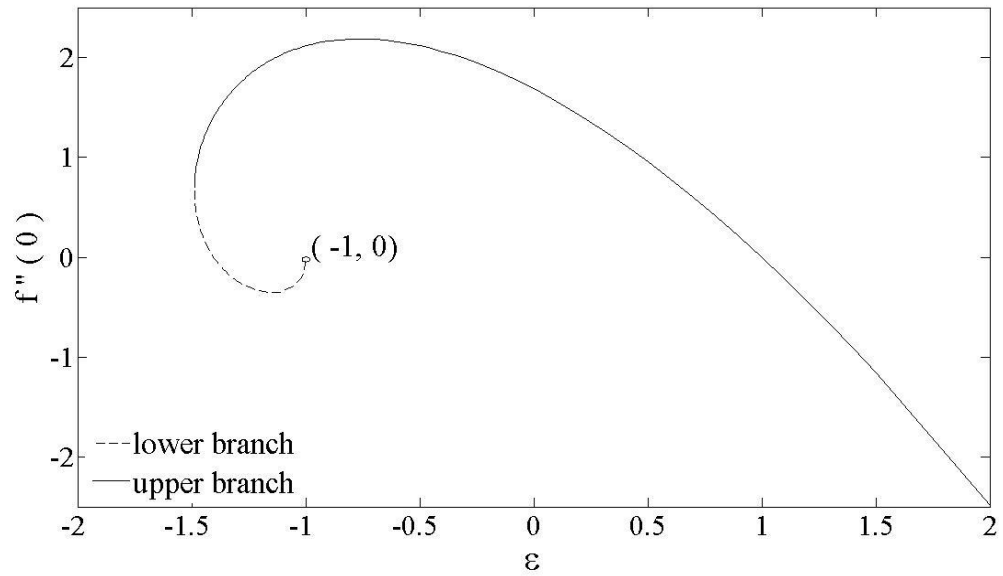


Figure 3.2 Variation of the skin friction coefficient $f''(0)$ with ε

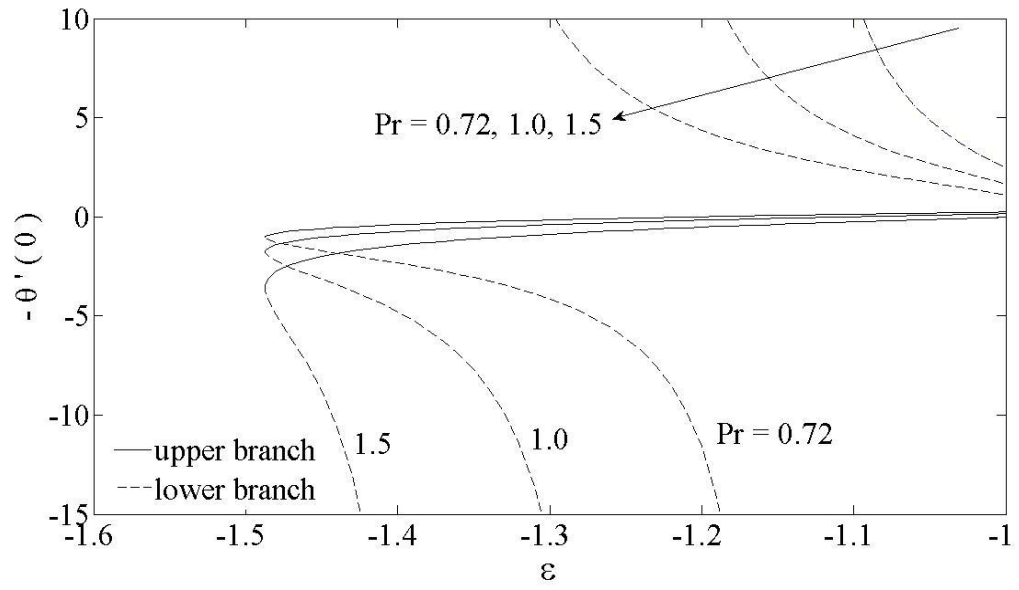


Figure 3.3 Variation of the local Nusselt number $-\theta'(0)$ with ε for various values of Pr

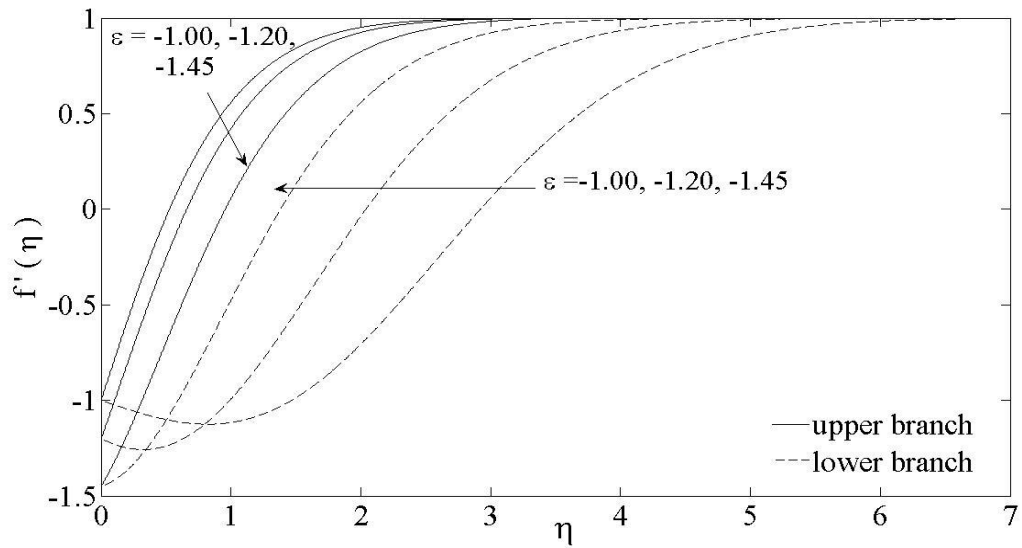


Figure 3.4 Velocity profile $f'(\eta)$ for various values of $\varepsilon < 0$

Figure 3.5 shows the effects of $\varepsilon < 0$ (shrinking) on the temperature profiles when $Pr = 1$. For the upper branch solution, with increasing negative values of ε , the temperature gradient at the surface increases, resulting in an increase of the local Nusselt number. The opposite trend is observed for the lower branch solution, increasing ε (in absolute sense) is to decrease the temperature gradient at the surface.

The temperature profiles for different values of Pr when $\varepsilon = -1.45$ are presented in Figure 3.6. It is seen that the temperature gradient at the surface increases as Pr increases. Thus, the local Nusselt number $-\theta'(0)$, which represents the heat transfer rate at the surface increases (in absolute sense) as the Prandtl number Pr increases.

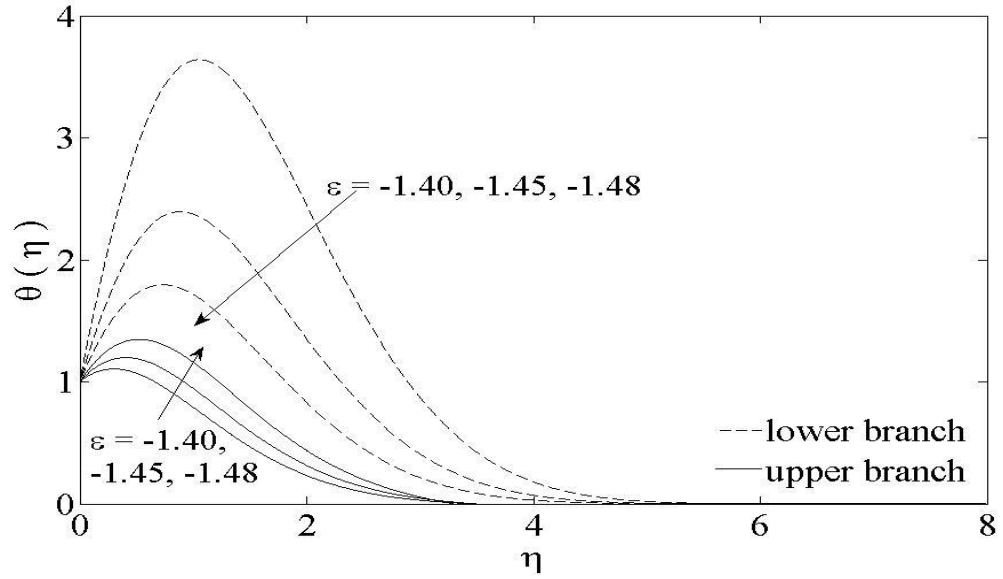


Figure 3.5 Temperature profile $\theta(\eta)$ for various values of $\varepsilon < 0$ when $Pr = 1$

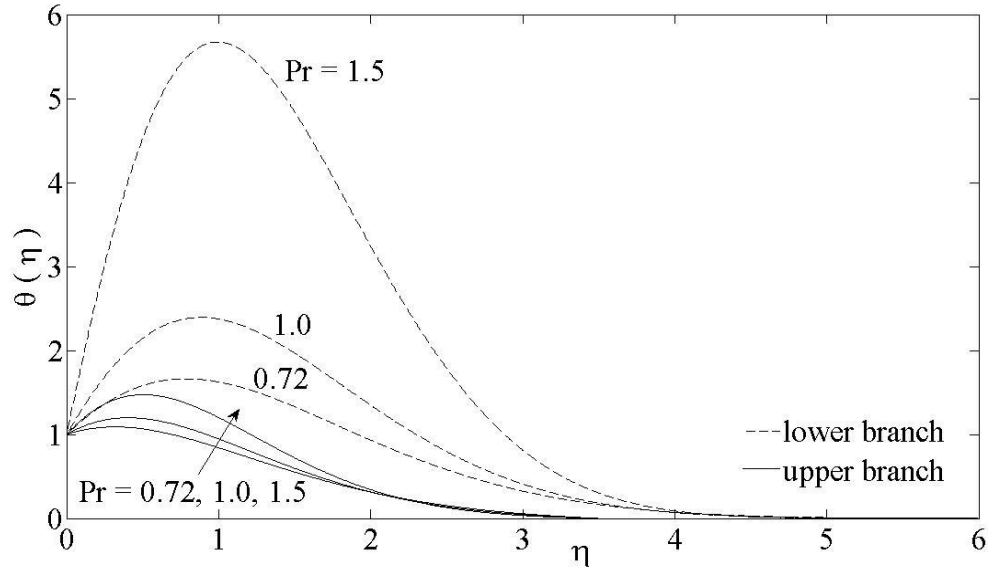


Figure 3.6 Temperature profile $\theta(\eta)$ for various values of Pr when $\varepsilon = -1.45$

The temperature overshoot shown in Figures 3.5 and 3.6 stems from the balancing act between the heat transfer from the solid boundary and its diffusion into the boundary layer and convection from the moving flows. It is dependent upon the Prandtl number Pr and the stretching/shrinking parameter ε . If the production of heat (heat transfer and diffusion) is greater than the convection term, then there will be accumulation of heat and thus the increase of temperature. For the stretching case, there is no temperature overshoot, as shown in Figures 3.7 and 3.8. Both Figures 3.7 and 3.8 show that increasing Pr or ε is to decrease the thermal boundary layer thickness, and in consequence increases the local Nusselt number $-\theta'(0)$. Thus, the heat transfer rate at the surface increases as Pr or ε increases.

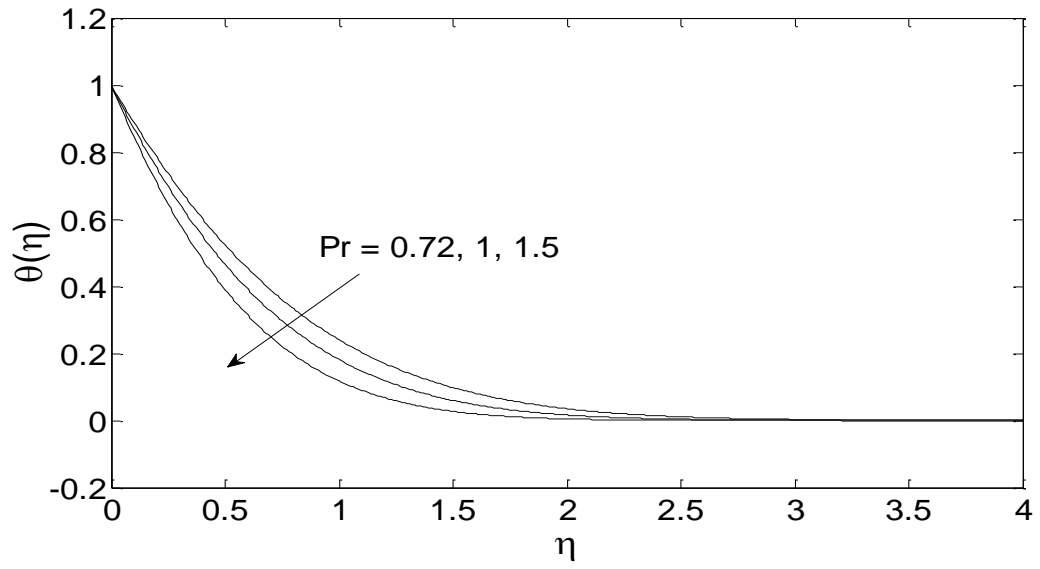


Figure 3.7 Temperature profile $\theta(\eta)$ for various values of Pr when $\varepsilon = 0.5$

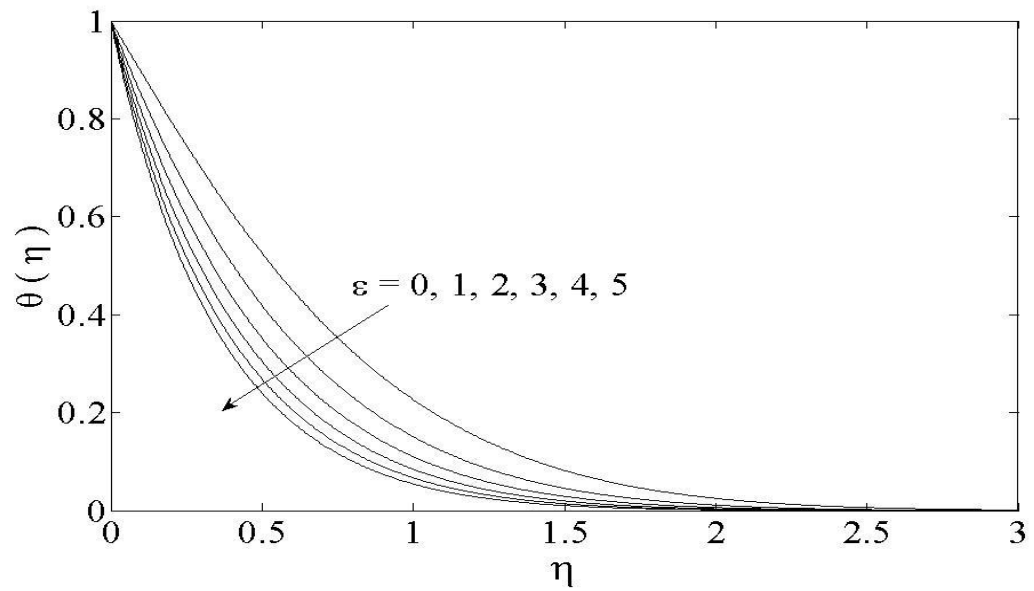


Figure 3.8 Temperature profile $\theta(\eta)$ for various values of ε when $Pr = 1$

The velocity profiles for selected values of $\varepsilon (\geq 0)$ are presented in Figure 3.9. This figure shows that the velocity gradient at the surface is zero when $\varepsilon = 1$, positive when $\varepsilon < 1$, and negative when $\varepsilon > 1$. This observation is in agreement with the results presented in Figure 3.2. We also note that the velocity boundary layer thickness decreases as ε increases. Finally, the velocity and temperature profiles for selected values of parameters presented in Figures 3.4-3.9 show that the far field boundary conditions (3.8) are satisfied asymptotically, thus supporting the validity of the numerical results obtained, besides supporting the dual nature of the solutions to the boundary value problem (3.6)-(3.8).

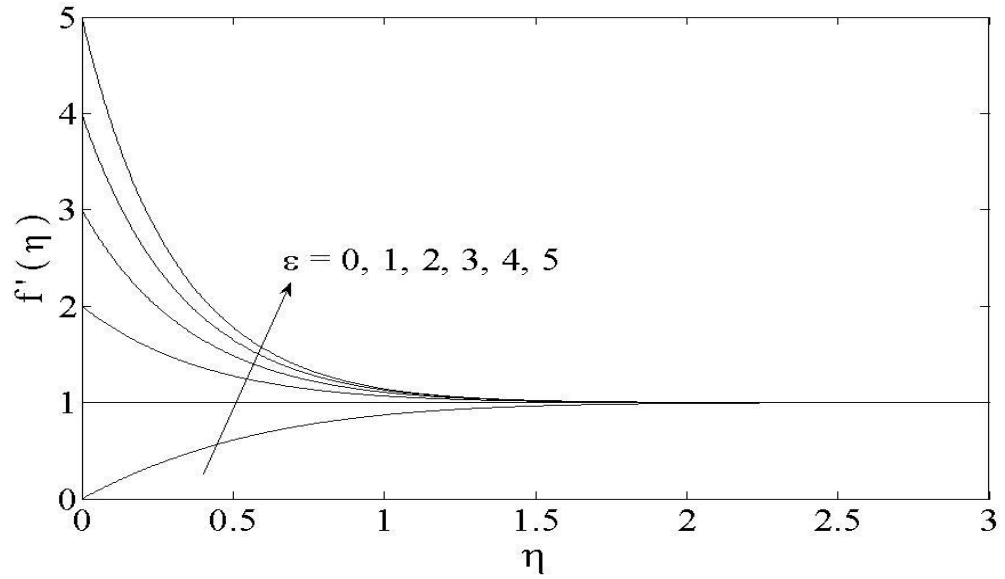


Figure 3.9 Velocity profile $f'(\eta)$ for various values of ε

3.4 Conclusions

The problem of stagnation-point flow over an exponentially shrinking/stretching sheet immersed in an incompressible viscous fluid was investigated numerically. Similarity solutions were obtained, and the effects of the governing parameters, namely the shrinking/stretching parameter ε and the Prandtl number Pr on the fluid flow and heat transfer characteristics were discussed. It was found that dual solutions exist for the shrinking case, while for the stretching case, the solution is unique. Moreover, it was found that increasing the Prandtl number is to increase the heat transfer rate at the surface.

CHAPTER 4

BOUNDARY LAYER FLOW AND HEAT TRANSFER OVER AN EXPONENTIALLY STRETCHING/SHRINKING PERMEABLE SHEET WITH VISCOUS DISSIPATION

4.1 Introduction

The study of fluid flow over a stretching/shrinking sheet has diverse technological applications in industrial processes. Many of the industrial manufacturing processes involve material sheeting production in metal or polymer sheet (Altan et al. 1983; Fisher 1976). For instance, manufacturing of glass fiber, drawing of plastic sheets, polymer melts, metallic plate in a cooling bath, and the cooling and drying of papers. The quality of the final products depends heavily on the rate of heat transfer at the stretching or shrinking surface (Karwe & Jaluria 1988).

For these applications, Crane (1970) was one of the earlier pioneers to discuss two-dimensional steady flow of an incompressible viscous fluid over a stretching sheet. He gave a closed form solution for the boundary layer flow on a moving plate. Chen (1998) analyzed the effect of thermal buoyancy forces on mixed convection boundary layer flow pass a stretching sheet, where the temperature varies in a power law form. He reported that the buoyancy force parameter induced the surface heat transfer rate. Similar fluid flows induced by stretching sheet have been considered by several researchers in various aspects (see Ishak et al. 2006b, 2007; Ishak 2009; Bataller 2008a, 2008b; Weidman & Ali 2011).

Besides the flow due to a stretching sheet as discussed, our objective is also to discuss the flow and heat transfer characteristics that are brought about by the shrinking sheet. This type of flows has been considered by several authors. One of the earlier fluid flows of this nature was first discussed by Miklavčič and Wang (2006). Their numerical solution becomes non-unique after some critical mass suction s . For stretching sheet, previous studies (Gupta & Gupta 1977) show that the solutions are unique for all suction rates. Later, Wang (2008) studied the effects of axisymmetric stagnation point flow over a shrinking/stretching sheet in power-law form. The axisymmetric case shows that for shrinking with suction rate $s < -1.2465$, no solution exists.

However, there are other various interesting studies in stretching or shrinking cases. Van Gorder and Vajravelu (2011) studied second grade fluid flows over an exponentially stretching or shrinking surface which admits an explicit exact solution. Van Gorder (2010) also investigated the nonlinear boundary value problems inclusive of mass transfer with exponentially decaying solution and provided the criterion for the existence of single and multiple solutions. Fang and Zhang (2009) obtained exact solution for MHD flow over a linear shrinking sheet with suction and injection. Multiple solution branches were observed for certain mass suction parameter. Later, Fang et al. (2009) considered unsteady flow through shrinking sheet in porous medium. They showed that for mass suction $s > 2$, the solution exists. Recently, researchers such as Cortell (2010), Noor et al. (2010), Fang et al. (2010), Merkin and Kumaran (2010) and Ishak et al. (2010a) have numerically studied the flow induced by a shrinking sheet with diversely different features, for example micropolar fluid, unsteady state, MHD and second order slip flows.

Motivated by the above investigations, we study the boundary layer flow and heat transfer over an exponentially stretching/shrinking permeable sheet with viscous dissipation. The skin friction coefficient and the local Nusselt number are determined for the flow field and the thermal field, respectively.

4.2 Problem Formulation

Consider a steady two-dimensional boundary layer flow and heat transfer of a viscous and incompressible fluid over an exponentially stretching/shrinking permeable sheet as shown in Figure 4.1. The Cartesian coordinates (x, y) are taken such that the x -axis is measured along the sheet oriented in the horizontal direction and the y -axis is perpendicular to it.

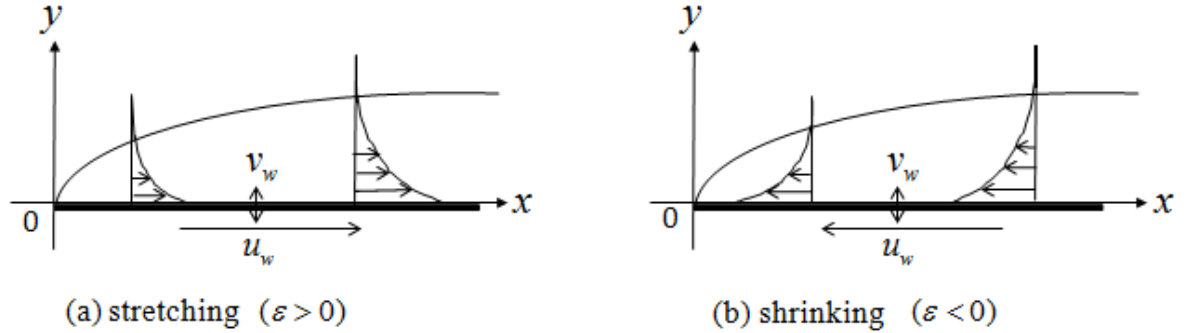


Figure 4.1 Physical model and coordinate system

It is assumed that the velocity of the stretching/shrinking sheet is $u_w(x) = U_w \exp(x/L)$, the surface temperature is $T_w(x) = T_\infty + T_0 \exp(2x/L)$ and the ambient uniform temperature is T_∞ , where L is the reference length and $T_0 > 0$. Under the boundary layer approximations, the governing equations of continuity, momentum and energy are

$$\frac{\partial u}{\partial x} + \frac{\partial v}{\partial y} = 0, \quad (4.1)$$

$$u \frac{\partial u}{\partial x} + v \frac{\partial u}{\partial y} = \nu \frac{\partial^2 u}{\partial y^2}, \quad (4.2)$$

$$\rho C_p \left(u \frac{\partial T}{\partial x} + v \frac{\partial T}{\partial y} \right) = k \frac{\partial^2 T}{\partial y^2} + \mu \left(\frac{\partial u}{\partial y} \right)^2, \quad (4.3)$$

subject to the boundary conditions

$$\begin{aligned} u = \pm u_w(x), \quad v = v_w(x), \quad T = T_w(x) \quad \text{at } y = 0, \\ u \rightarrow 0, \quad T \rightarrow T_\infty \quad \text{as } y \rightarrow \infty, \end{aligned} \quad (4.4)$$

where + and – signs correspond to a stretching and a shrinking sheet, respectively, ν is the kinematic viscosity, ρ the fluid density, C_p the specific heat at constant pressure, k the thermal conductivity and μ is the dynamic viscosity.

To obtain similarity solution, we introduce the following similarity variables:

$$\begin{aligned} \psi = \sqrt{2\nu L U_w} \exp\left(\frac{x}{2L}\right) f(\eta), \quad \theta(\eta) = (T - T_\infty)/(T_w - T_\infty), \\ \eta = y \sqrt{\frac{U_w}{2\nu L}} \exp\left(\frac{x}{2L}\right), \end{aligned} \quad (4.5)$$

where ψ is the stream function defined as $u = \partial\psi / \partial y$ and $v = -\partial\psi / \partial x$, which identically satisfies Equation (4.1). By this definition, we obtain

$$u = U_w \exp\left(\frac{x}{L}\right) f'(\eta), \quad v = -\sqrt{\frac{\nu U_w}{2L}} \exp\left(\frac{x}{2L}\right) [f(\eta) + \eta f'(\eta)] \quad (4.6)$$

where prime denotes differentiation with respect to η . Further, to obtain similarity solution, we take

$$v_w(x) = -\sqrt{\frac{\nu U_w}{2L}} \exp\left(\frac{x}{2L}\right) s \quad (4.7)$$

where $s = f(0)$ is a constant: $s > 0$ corresponds to suction, $s < 0$ corresponds to injection or blowing, $s = 0$ corresponds to an impermeable surface.

Substituting (4.5) and (4.6) into Equations (4.2) and (4.3), we obtain the following system of nonlinear ordinary differential equations:

$$f''' + ff'' - 2f'^2 = 0, \quad (4.8)$$

$$\frac{1}{\text{Pr}} \theta'' + f\theta' - 4f'\theta + \text{Ec}f''^2 = 0. \quad (4.9)$$

The boundary conditions (4.4) then become

$$\begin{aligned} f(0) &= s, & f'(0) &= \varepsilon, & \theta(0) &= 1, \\ f'(\eta) &\rightarrow 0, & \theta(\eta) &\rightarrow 0 & \text{as } \eta &\rightarrow \infty, \end{aligned} \quad (4.10)$$

where $\varepsilon = \pm 1$ is the stretching/shrinking parameter, Pr is the Prandtl number and Ec is the Eckert number, which are defined as

$$\text{Pr} = \frac{\mu C_p}{k}, \quad \text{Ec} = \frac{U_w^2}{T_0 C_p}. \quad (4.11)$$

Here $\varepsilon = 1$ denotes stretching sheet whilst $\varepsilon = -1$ is a shrinking sheet.

The main physical characteristics of interest in the present problem are the skin friction coefficient C_f and the local Nusselt number Nu_x , which are defined as

$$C_f = \frac{\tau_w}{\rho u_w^2}, \quad Nu_x = \frac{x q_w}{k(T_w - T_\infty)}, \quad (4.12)$$

respectively, where the surface shear stress τ_w and the surface heat flux q_w are given by

$$\tau_w = \mu \left(\frac{\partial u}{\partial y} \right)_{y=0}, \quad q_w = -k \left(\frac{\partial T}{\partial y} \right)_{y=0}. \quad (4.13)$$

Substituting (4.5) into Equations (4.12) give

$$\left(\frac{2L}{x} \right)^{\frac{1}{2}} C_f \text{Re}_x^{1/2} = f''(0), \quad \left(\frac{2L}{x} \right)^{\frac{1}{2}} Nu_x \text{Re}_x^{-1/2} = -\theta'(0) \quad (4.14)$$

where $\text{Re}_x = u_w x / \nu$ is the local Reynolds number.

4.3 Results and Discussion

Numerical results are presented for different physical parameters. Since the flow problem is uncoupled from the thermal problem, changes in the values of Pr and Ec will not affect the fluid velocity. Therefore, Pr and Ec are considered unity throughout this chapter except where stated in the graph. Typical dimensionless stream function and the streamlines for $\varepsilon = 1$ (stretching) are shown in Figures 4.2a and 4.2b, respectively.

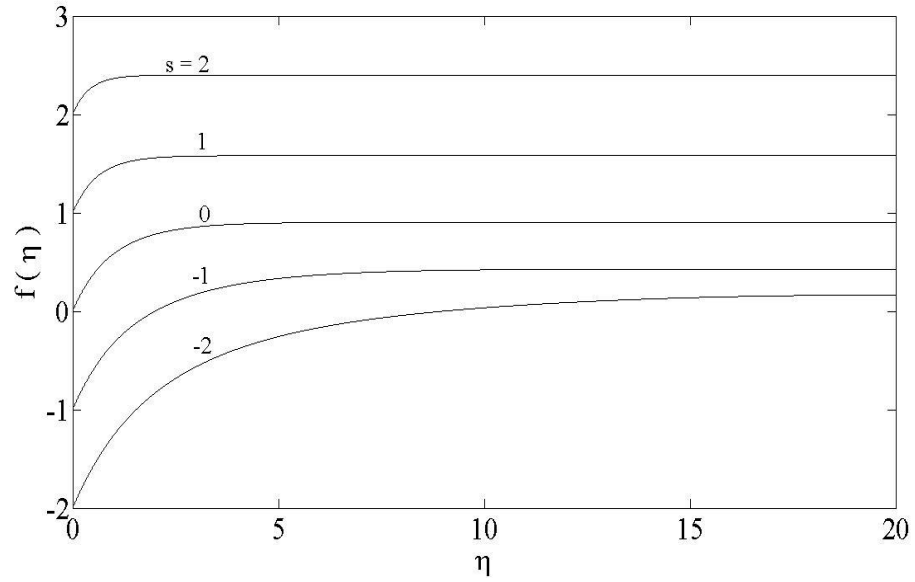


Figure 4.2a Dimensionless stream function $f(\eta)$ for various values of s when $\varepsilon = 1$

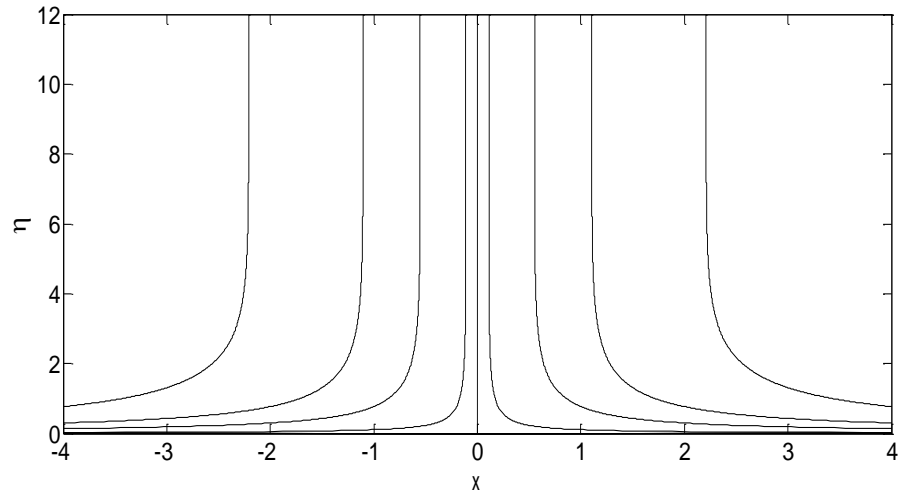


Figure 4.2b Streamlines for $s = 0$ and $\varepsilon = 1$

4.3.1 Stretching Case, $\varepsilon = 1$

Figure 4.3 shows the skin friction coefficient $f''(0)$ against suction/injection parameter s . We see that increasing the suction ($s > 0$) increases the magnitude of the skin friction coefficient, while injection acts in the opposite manner. Thus, the drag force is larger for suction compared to injection.

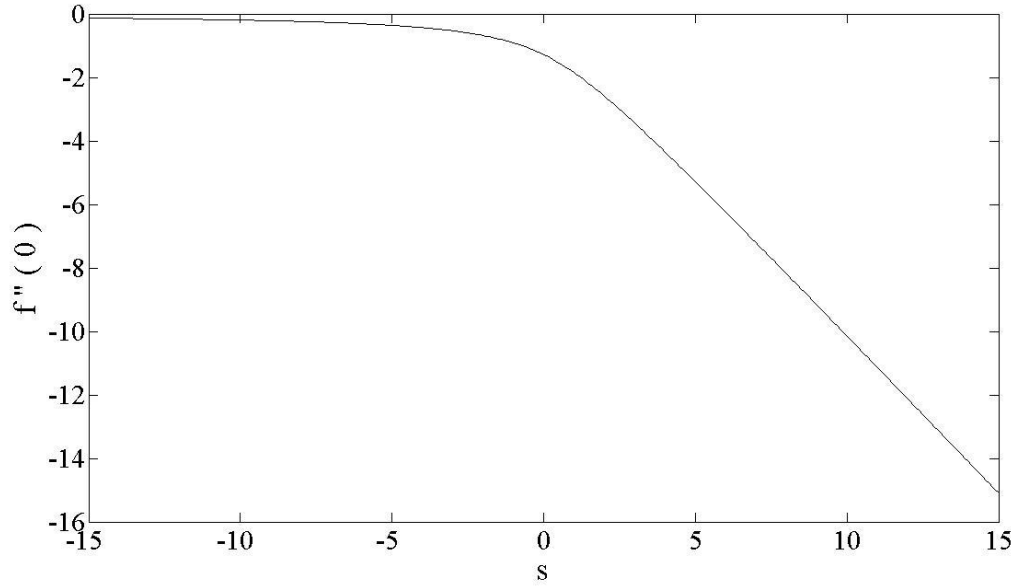


Figure 4.3 Variation of the skin friction coefficient $f''(0)$ with s when $\varepsilon = 1$

Figures 4.4 and 4.5 display the variations of the local Nusselt number $-\theta'(0)$ with s for some values of Prandtl number Pr and Eckert number Ec , respectively. Both figures clearly show the significant effects of Pr and Ec toward Nusselt number respectively as s increases. In Figure 4.4 the local Nusselt number, which represents the heat transfer rate at the surface, increases with increasing Pr . Note that as $s \rightarrow -\infty$, $-\theta'(0) \rightarrow 0.0513$. However, in Figure 4.5 the heat transfer rate at the surface decreases to a minimum value when Ec is increasing; in fact as $s \rightarrow -\infty$, $-\theta'(0) \rightarrow 0.06975$ for all Ec number considered. This is due to viscous dissipation.

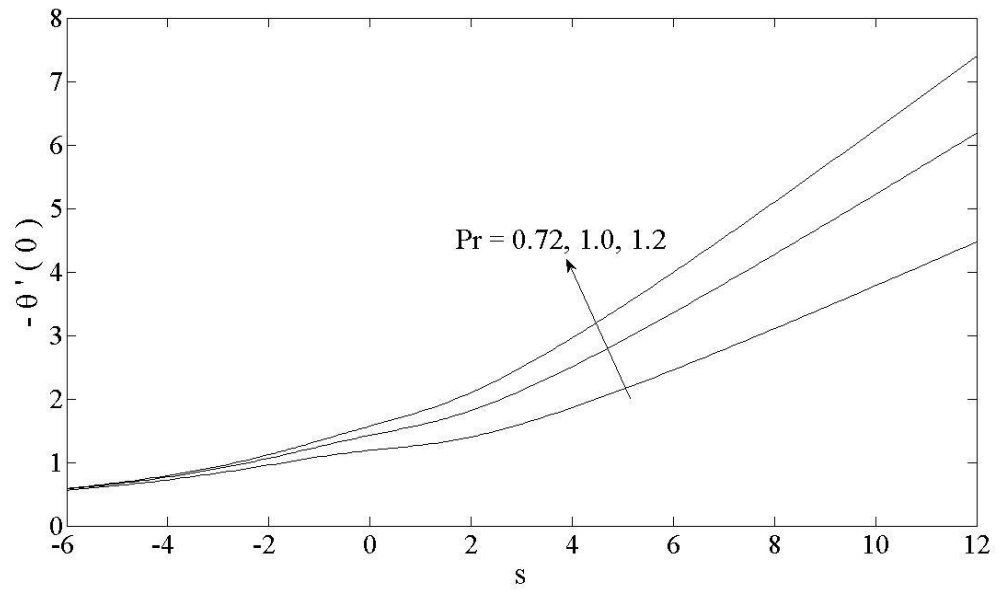


Figure 4.4 Variation of the local Nusselt number $-\theta'(0)$ with s for various values of Pr when $\varepsilon = 1$ and $Ec = 1$

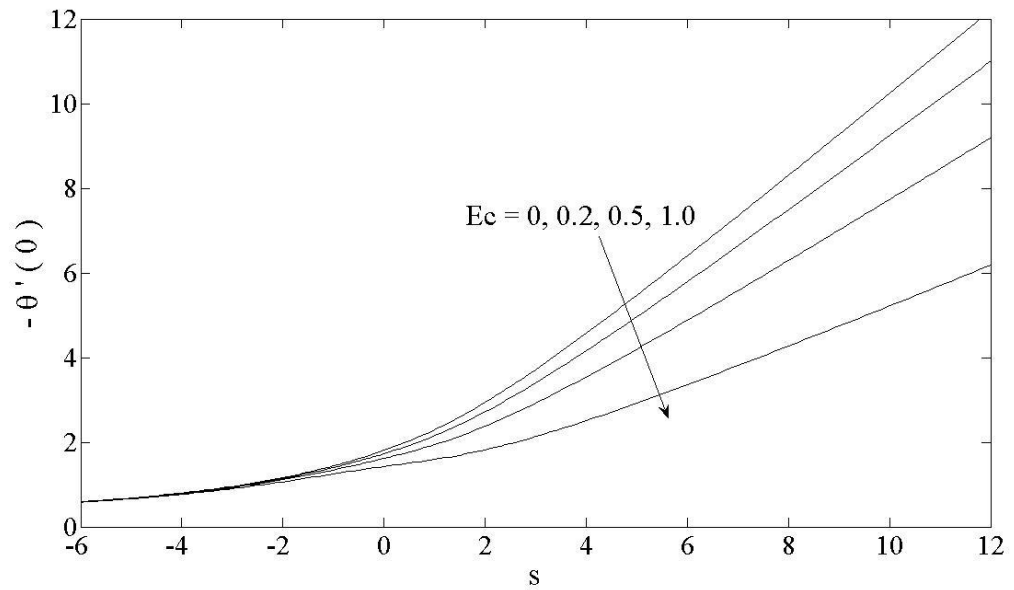


Figure 4.5 Variation of the local Nusselt number $-\theta'(0)$ with s for various values of Ec when $\varepsilon = 1$ and $Pr = 1$

Further, Figure 4.6 illustrates the velocity profile $f'(\eta)$ for various values of s . At any fixed η , it is found that when s increases the velocity $f'(\eta)$ decreases. This implies that the boundary layer thickness decreases as s increases. Figure 4.7 shows the temperature profiles $\theta(\eta)$ for various values of s . It can be seen that as s increases the thermal boundary layer thickness becomes thinner. This implies the temperature gradient at the surface increases as s increases. Thus the heat transfer rate at the surface increases as s increases, which is consistent with the result presented in Figure 4.4.

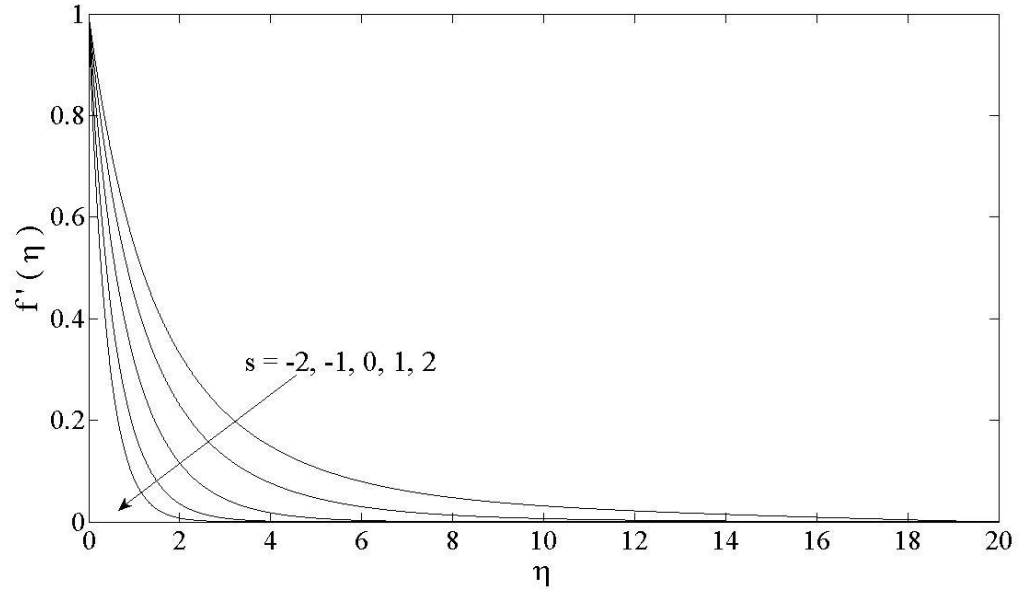


Figure 4.6 Velocity profile $f'(\eta)$ for various values of s when $\varepsilon = 1$

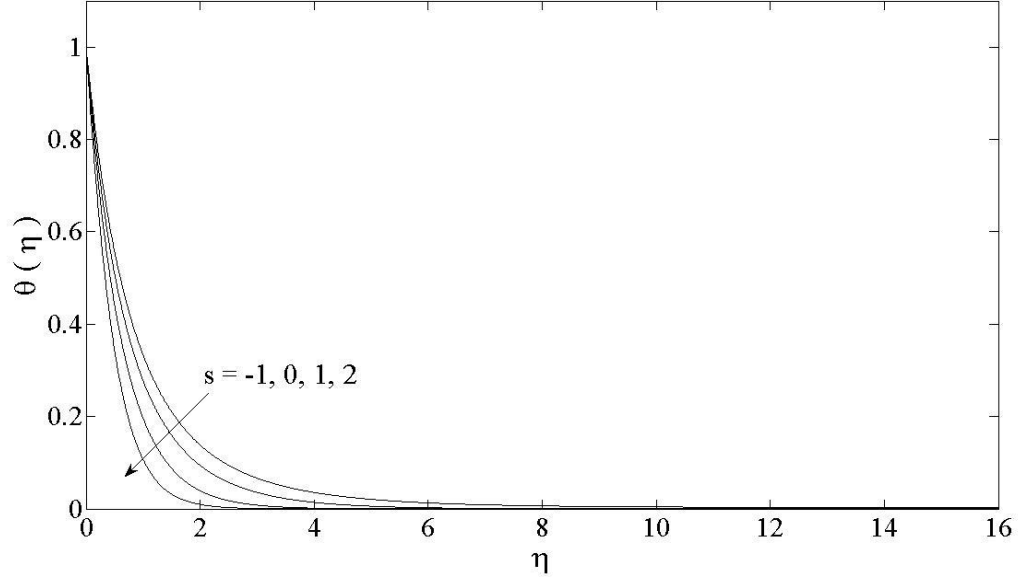


Figure 4.7 Temperature profile $\theta(\eta)$ for various values of s when $\varepsilon = 1, \text{Pr} = 1$ and $\text{Ec} = 1$

4.3.2 Shrinking Case, $\varepsilon = -1$

For shrinking boundary, the behaviors of the graphical results are dramatically different from the stretching boundary. Figure 4.8 shows the profile for the skin friction coefficient $f''(0)$ when s is positive (suction). In this figure, we note that two branches of solutions are found. The solid lines are the upper branch solutions and the dash lines are the lower branch solutions. We define the upper branch solutions by how they appear in Figure 4.8, i.e. the upper branch solution has a higher value of $f''(0)$ for a given s than the lower branch solution. As can be seen in Figure 4.8, there exist a critical value $s = s_c$ such that for $s < s_c$ there will be no solution, while dual solutions exist for $s > s_c$. Our numerical results show that $s_c \cong 2.1278$. The solutions bifurcate at $s = s_c > 0$ and form upper and lower branches. For the upper branch, solution exists for larger values of s than shown in Figure 4.8, whereas for the lower branch, solution exists up to $s \cong 5.7024$. It is worth mentioning that the computations have been performed until the solution does not

converge, and was terminated at that point. The dual solutions exhibit the normal forward flow behavior and the other is reversed flow where $f'(\eta) < 0$. It is observed that solutions only exist for certain wall suction value; no solution exists with wall injection. Therefore, suction plays an important role to maintain the existence of solution of fluid flow in shrinking boundary.

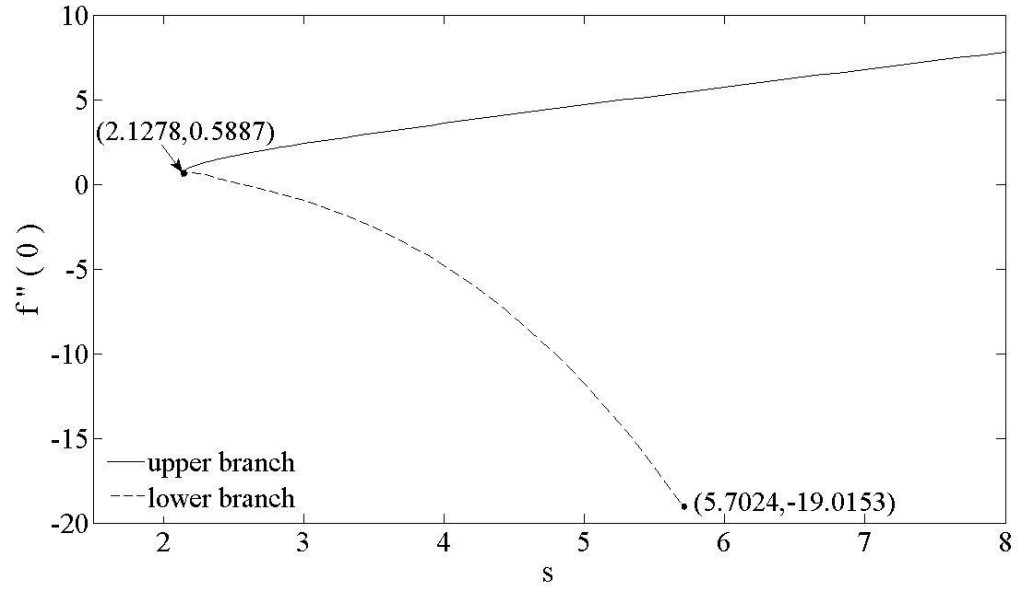


Figure 4.8 Variation of the skin friction coefficient $f''(0)$ with s when $\varepsilon = -1$

Figures 4.9-4.10 display the variations of the local Nusselt number $-\theta'(0)$ with s for various values of Pr and Ec , respectively. In these figures, for the lower branch solutions, it is clear that the heat transfer rate at the surface tends to $-\infty$ as it approaches $s \approx 2.33$ from the left, and tends to $+\infty$ from the right. Thus, we expect that the lower branch solution is not physically relevant. Figure 4.9 shows that for the upper branch solutions, the heat transfer rate at the surface increases as Pr increases when $s > 2.5$. It is noted that positive value of $-\theta'(0)$ denotes the heat is transferred from the sheet to the

fluid and vice versa. On the other hand, in Figure 4.10 for the upper branch solution it can be seen that at any chosen η the value of $-\theta'(0)$ decreases as Eckert number increases. The bifurcation points $(s_c, -\theta'(0))$ for Figures 4.9 and 4.10 are given in Table 4.1. It is worth mentioning to this end that as in similar physical situations, we postulate that the upper branch solutions are physically stable and occur in practice, whilst the lower branch solutions are not physically realizable. This postulate can be verified by performing a stability analysis but this is beyond the scope of the present study. However, the interested reader can find the procedure for showing this in the papers by Merkin (1985), Weidman et al. (2006), Harris et al. (2009), Mahapatra et al. (2011) and Postelnicu and Pop (2011). A snapshot of the $\theta(\eta)$ variation for various values of Pr and Ec when $s = 2.3$ can be seen in Figures 4.11 and 4.12 respectively.

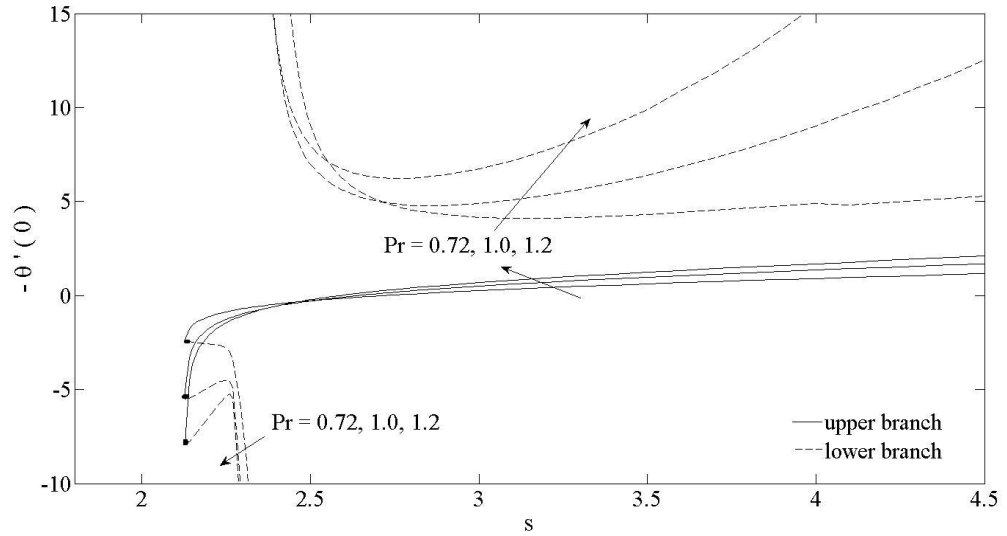


Figure 4.9 Variation of the local Nusselt number $-\theta'(0)$ with s for various values of Pr when $\varepsilon = -1$ and $Ec = 1$

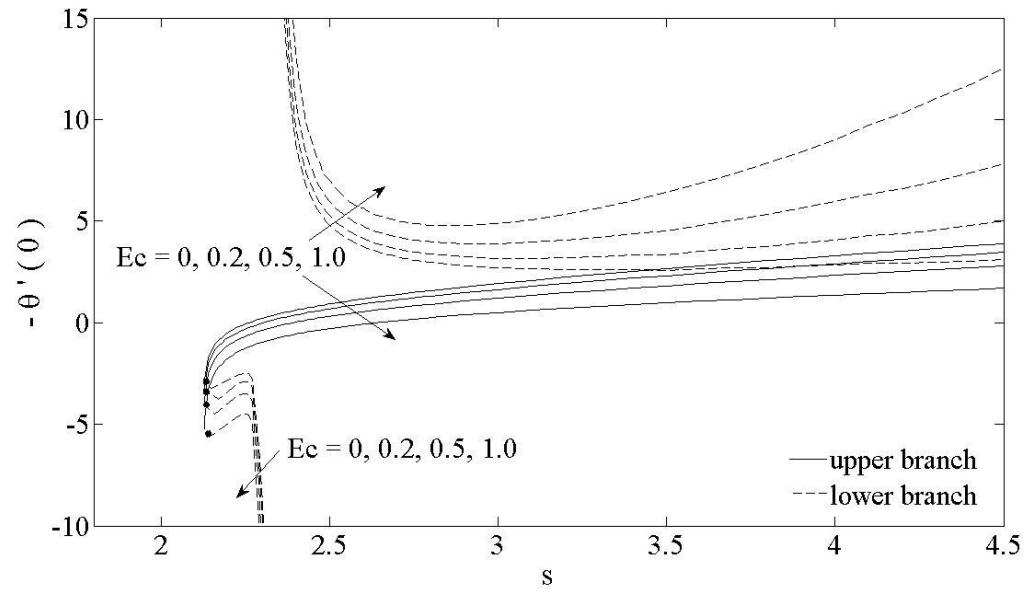


Figure 4.10 Variation of the local Nusselt number $-\theta'(0)$ with s for various values of Ec when $\varepsilon = -1$ and $Pr = 1$

Table 4.1 Values of $-\theta'(0)$ for bifurcation points in Figures 4.9 and 4.10

Ec	Pr	s	$-\theta'(0)$
1	0.72	2.1278	-2.3153
	1.0	2.1278	-4.9595
	1.2	2.1278	-7.7316
0	1	2.1278	-2.9139
0.2		2.1278	-3.3230
0.5		2.1278	-3.9367
1.0		2.1278	-4.9595

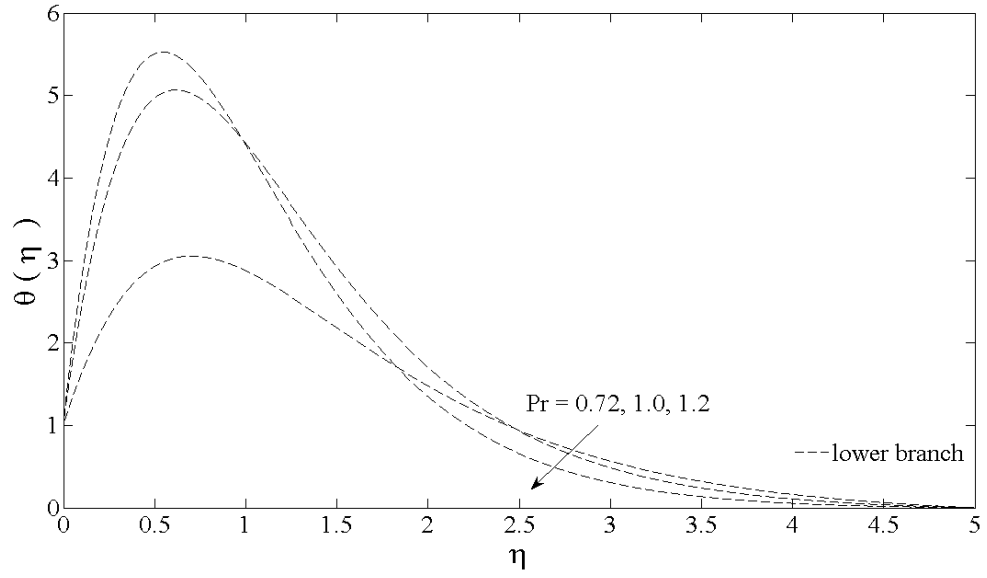


Figure 4.11 Temperature $\theta(\eta)$ variation, with $s = 2.3$ and $Ec = 1$, for various values of Pr when $\varepsilon = -1$.

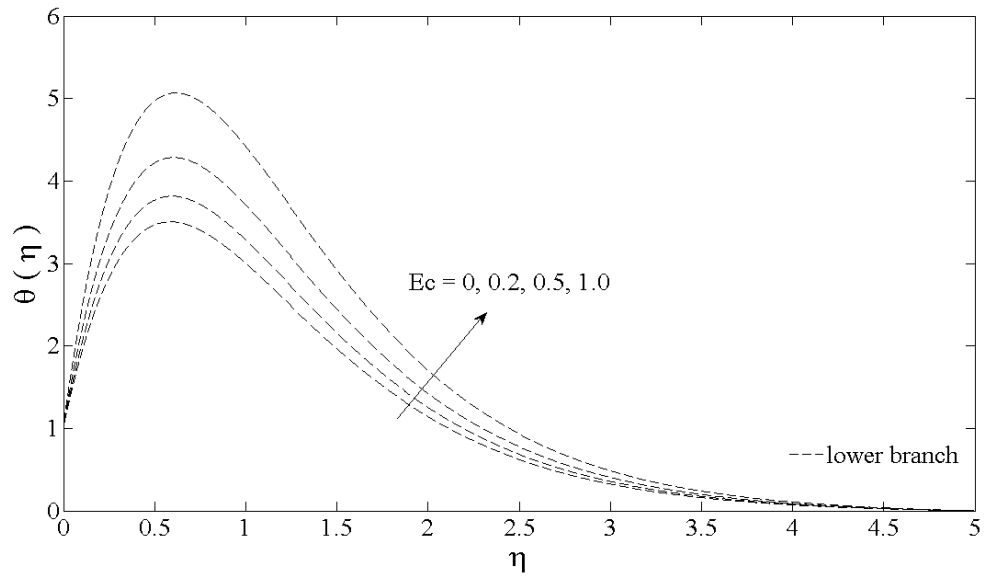


Figure 4.12 Temperature $\theta(\eta)$ variation, with $s = 2.3$ and $Pr = 1$, for various values of Ec when $\varepsilon = -1$.

We now consider the characteristics of dimensionless velocity and temperature profiles in shrinking boundary layer as shown in Figures 4.13 and 4.14, respectively. In Figure 4.13 it is clear that the upper branch solutions have a positive velocity gradient in the neighbourhood of the surface, whereas for the lower branch solutions the velocity gradient is negative when $s > 2.619$. This implies that above the sheet there exist a region of reversed flow. This result agrees well with the existence of dual solutions in Figure 4.8. In Figure 4.14, for any fixed station η the upper branch temperature profile decreases as s increases, whilst for the lower branch solutions there exist a minimum negative value of temperature $\theta(\eta)$ for the respective s . Since the temperature $\theta(\eta)$ is always positive by definition, see Equation (4.5), the lower branch temperature solution is physically unrealistic. Thus for realistic boundary layer and temperature solutions, these lower branch solutions must be disregarded. Although such solutions are deprived of physical significant, they are nevertheless of interest as far as differential equations are concerned (Rhida 1996).

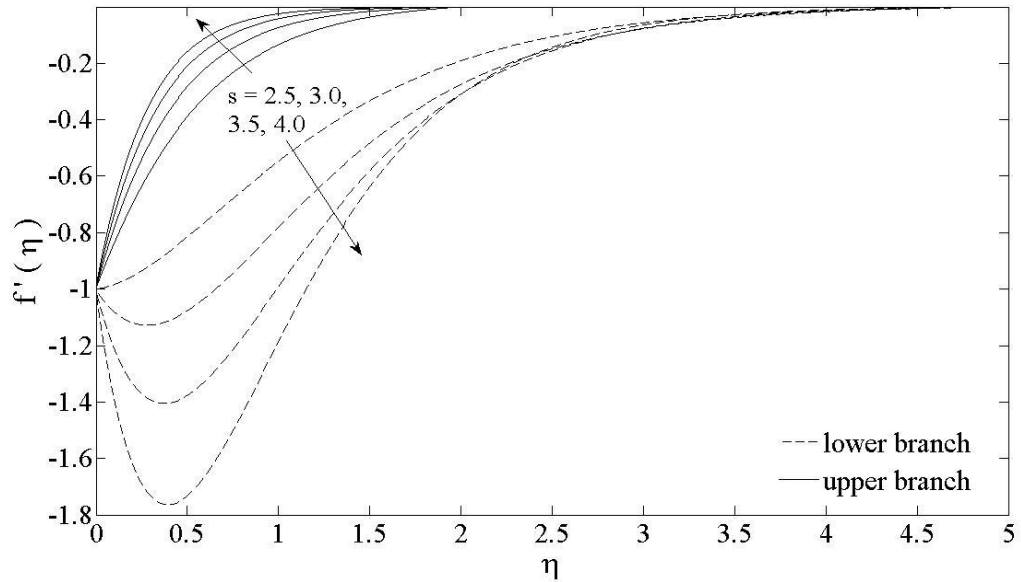


Figure 4.13 Velocity profile $f'(\eta)$ for various values of s when $\varepsilon = -1$

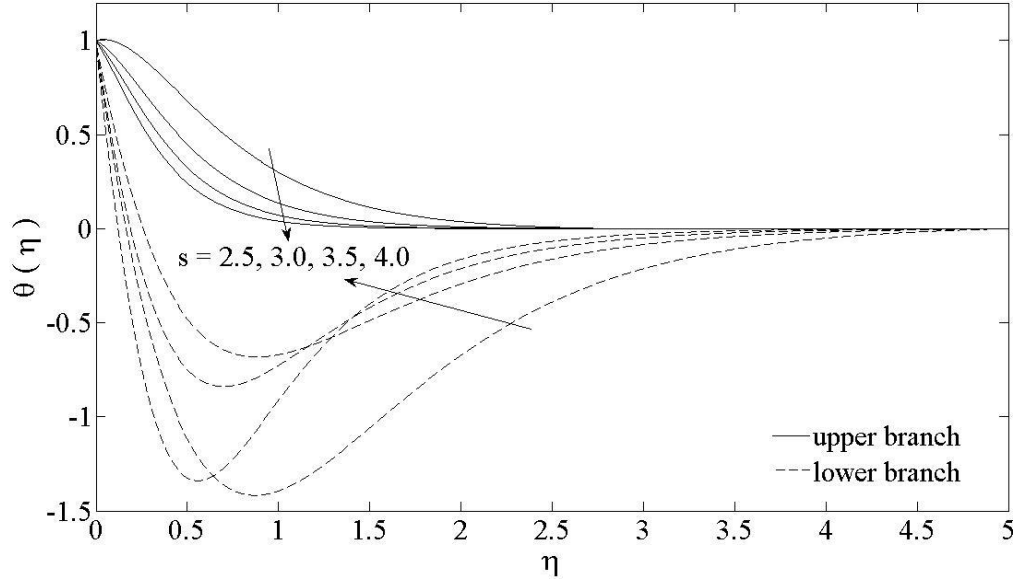


Figure 4.14 Temperature profile $\theta(\eta)$ for various values of s when $\varepsilon = -1, \text{Pr} = 1$, and $Ec = 1$

The velocity and temperature profiles for $s = 3.5$ when $\varepsilon = \pm 1$ are presented in Figures 4.15 and 4.16, respectively. Both profiles show existence of dual solutions for the boundary layer induced by a shrinking sheet. It can be seen that all of these solutions profiles approach the far field boundary condition (4.10) asymptotically; thus supporting the numerical results obtained.

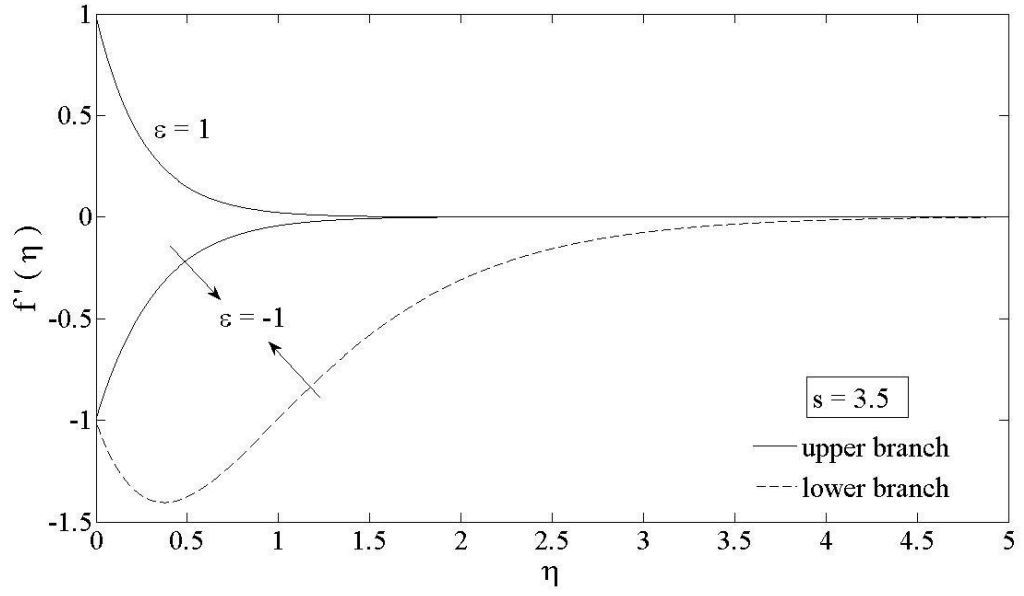


Figure 4.15 Velocity profile $f'(\eta)$ when $s = 3.5$ for $\epsilon = \pm 1$

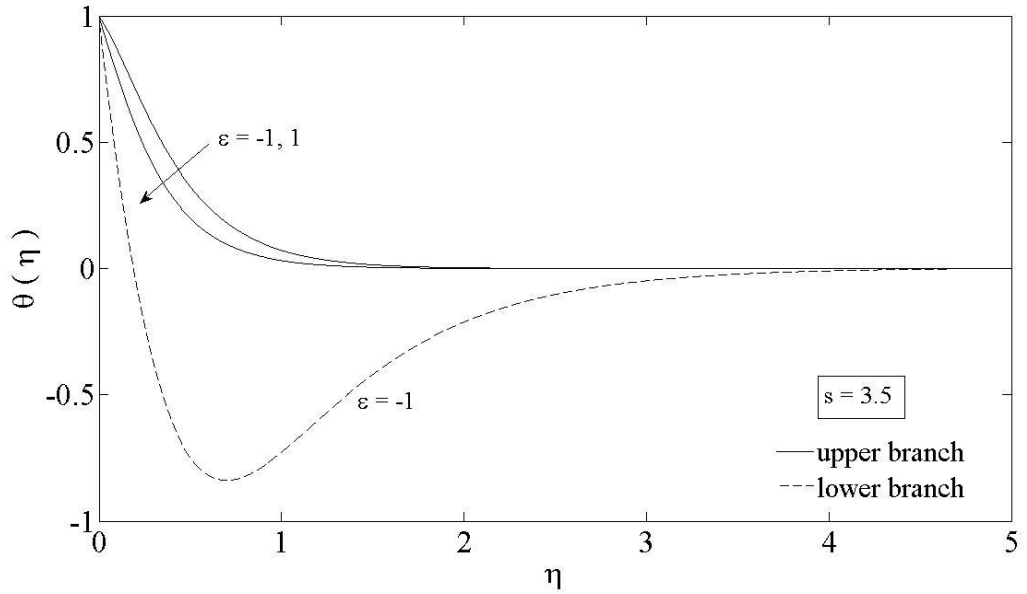


Figure 4.16 Temperature profile $\theta(\eta)$ for $\epsilon = \pm 1$ when $s = 3.5$, $Pr = 1$, $Ec = 1$

4.4 Conclusions

The problem of boundary layer flow and heat transfer over an exponentially stretching/shrinking permeable sheet with viscous dissipation was investigated numerically. Similarity equations were obtained and solved numerically, and the effects of the governing parameters on the fluid flow and heat transfer characteristics were discussed. It was found that dual solutions exist for the shrinking boundary, while for the stretching boundary, the solution is always unique. Moreover, it was found that suction increases both the skin friction coefficient and the heat transfer rate at the surface.

CHAPTER 5

CONCLUSIONS AND FUTURE WORK

In this thesis, we have studied the viscous fluid flows and heat transfer boundary layer problems over a stretching or shrinking sheet. We have derived the general equations for fluid motion and heat transfer from the laws of conservation of mass, linear and angular momentum and energy in Chapter 1. Under the assumption of Prandtl's boundary layer theory and order of magnitude analysis, as well as focusing on steady state and two dimensional problems, the set of nonlinear PDE Navier-Stokes equations are reduced to steady, two-dimensional incompressible boundary layer fluid flows and heat transfer equations. Later, we have made use of the similarity transformation to reduce the governing boundary layer partial differential equations to a system of nonlinear ordinary differential equations. Therefore these resulting nonlinear systems of ODEs are now amenable to be solved numerically. In this thesis our objective is to study flows and heat transfer rates in the vicinity of stagnation point. At this point the flow velocity is at its minimum whilst the heat transfer rate is at its maximum.

We used the Keller-box method, originally suggested by Keller (1970), to solve the reduced governing nonlinear ordinary differential equations. The method is second order and unconditionally stable. Central differences techniques are constructed to replace the derivatives and the resulting non-linear difference equations are linearised by Newton's method. Then the linearised equations are solved by the block tridiagonal elimination method. The Keller box method has been applied to the three different problems respectively in Chapter 2-4.

In Chapter 2, we studied the effect of buoyancy forces towards a stretching vertical sheet immersed in viscous fluid, with the sheet velocity given in power form. The far field velocity is also of the power form. The buoyancy forces are either of assisting or opposing the fluid motion in the boundary layer. From our calculations, for assisting buoyancy force, all solutions are unique. In the case of opposing buoyancy force, dual solutions are obtained up to a certain critical value λ_c . This critical value λ_c depends on the values of velocity exponent parameter m and the velocity ratio parameter ε . The higher the velocity exponent parameter m , the higher is this critical value λ_c . The value of λ_c also increases when the velocity ratio parameter ε increases.

In Chapter 3, we discussed the stagnation point flow over a stretching or shrinking sheet immersed in viscous fluid, with the sheet in the horizontal direction. The deduced boundary layer equations are decoupled. The sheet velocity, far field fluid velocity and surface temperature are given in exponential form. The stretching or shrinking parameter is given by ε , with $\varepsilon > 0$ denoting stretching and $\varepsilon < 0$ shrinking. Our results show that all solutions are unique for $\varepsilon > -1$, that is for all stretching and shrinking cases. For the shrinking case, dual solutions are obtained from $\varepsilon < -1$ up to a critical value $\varepsilon_c \approx -1.4872$. This agrees very well with the results of Bhattacharyya and Vajravelu (2011). For heat transfer rate our results show that for stretching rate $\varepsilon = 1$, the heat transfer rate increases as Prandtl Pr increases. This is also true for any other $\varepsilon > 0$. When $\varepsilon = 1$, the exact solution for the fluid velocity field is $f(\eta) = \eta$.

In Chapter 4, the above problem in Chapter 3 is extended to include the effects of mass transfer and viscous dissipation. The suction or injection parameter is given by s , with $s > 0$ denoting suction and $s < 0$ injection. From our calculation, for the stretching case, all solutions are unique for either suction or injection. However, in the shrinking case, dual solutions are obtained from $s \approx 5.7024$ down to a critical value $s_c \approx 2.1278$. No solution exists smaller than this critical value s_c , that is no solution exists for $s < s_c$ for injection case. This agrees very well with the results of Bhattacharyya (2011). For heat transfer rate, our calculations show that for stretching case, the heat transfer rate increases as Prandtl Pr increases. Whilst the heat transfer rate increases when Eckert Ec decreases.

Looking ahead, in this thesis we have successfully analyzed exponentially form forced convection boundary layer problem in Chapter 3 and also a similar problem in Chapter 4 but with mass transfer through the sheet. We can extend this idea of exponential form to the body temperature or temperature heat flux and then letting the created motion to settle down. This is free convection. But most problems of this nature are mixed convection. Thus free and mixed convection studies can be made in future investigation. The effects of magnetic field, porous medium, heat flux, slip condition, non-Newtonian fluids such as micropolar fluids can also be considered. However the current algorithms developed for solving the system of nonlinear ODEs in this study are second order accurate and the accuracy is found wanting. Apart from that, a systematics method not only to relate η_∞ and computational accuracy but also searching multisolutions and higher convergence should be looked into seriously. Therefore, a higher order accuracy algorithm and a more robust and stable scheme is needed to study these more delicate free and mixed convection problems.

REFERENCES

- Acheson, D. J. (1990). *Elementary fluid dynamics*. New York: Oxford University Press Inc.
- Ali, F. M., Nazar, R., Arifin, N. M., & Pop, I. (2011). Unsteady shrinking sheet with mass transfer in a rotating fluid. *International Journal for Numerical Methods in Fluids* 66:1465–1474.
- Altan, T., Oh, S. I., & Gegel, H. L. (1983). *Metal forming fundamentals and applications*. American Society for Metals, Metal Park, Ohio.
- Andersson, H. I., Back, K. H., & Dandapat, B. S. (1992). Magnetohydrodynamic flow of a power-law fluid over a stretching sheet. *International Journal of Non-Linear Mechanics* 27: 929-939.
- Bataller, R. C. (2008a). Radiation effects in the Blasius flow. *Applied Mathematics and Computation* 198:333-338.
- Bataller, R. C. (2008b). Similarity solution for flow and heat transfer of a quiescent fluid over a nonlinearly stretching surface. *Journal of Materials Processing Technology* 203:176-183.
- Bhattacharyya, K. (2011). Boundary layer flow and heat transfer over an exponentially shrinking sheet. *Chinese Physics Letters* 28:074701/
- Bhattacharyya, K., & Layek, G. C. (2011). Effects of suction/blowing on steady boundary layer stagnation-point flow and heat transfer towards a shrinking sheet with thermal radiation. *International Journal of Heat and Mass Transfer* 54:302-307.
- Bhattacharyya, K., & Vajravelu, K. (2011). Stagnation-point flow and heat transfer over an exponentially shrinking sheet. *Communications in Nonlinear Sciences and Numerical Simulation* 17:2728-2734.

- Bidin, B. & Nazar, R. (2009). Numerical solution of the boundary layer flow over an exponentially stretching sheet with thermal radiation. *European Journal of Scientific Research* 33:710 – 717.
- Chen, C. H. (1998). Laminar mixed convection adjacent to vertical, continuously stretching sheets. *Heat Mass Transfer* 33:471-476.
- Cortell, R. (2010). On a certain boundary value problem arising in shrinking sheet flows. *Applied Mathematics and Computation* 217:4086-4093.
- Crane, L. J. (1970). Flow past a stretching plane. *Journal of Applied Mathematics and Physics (ZAMP)* 21:645-647.
- Daily, J. W., & Harleman D. R. F. (1966). *Fluid Dynamics*. Reading, MA: Addison-Wesley, 1966.
- El-Aziz, M. A. (2009). Viscous dissipation effect on mixed convection flow of a micropolar fluid over an exponentially stretching sheet. *Canadian Journal of Physics* 87:359-368.
- Fang, T. (2008). Boundary layer flow over a shrinking sheet with power-law velocity. *International Journal of Heat and Mass Transfer* 51:5838-5843.
- Fang, T., Yao, S., Zhang, J., & Aziz, A. (2010). Viscous flow over a shrinking sheet with a second order slip flow model. *Communications in Nonlinear Science and Numerical Simulation* 15:1831-1842.
- Fang, T., & Zhang, J. (2009). Closed-form exact solution of MHD viscous flow over a shrinking sheet. *Communications in Nonlinear Science and Numerical Simulation* 14:2853-2857.
- Fang, T., Zhang, J., & Yoa, S. (2009). Viscous flow over an unsteady shrinking sheet with mass transfer. *Chinese Physics Letters* 26:014703.
- Fisher E.G. (1976). *Extrusion of Plastics*. Wiley: New York.

- Fourier, J. B. (1822). *Theorie Analytique de la Chaleur*. Didot, Paris.
- Gupta, P. S., & Gupta, A. S. (1977). Heat and mass transfer on a stretching sheet with suction or blowing. *The Canadian Journal of Chemical Engineering* 55:744-746.
- Harris, S. D., Ingham, D. B., & Pop, I. (2009). Mixed convection boundary-layer flow near the stagnation point on a vertical surface in a porous medium: Brinkman model with slip. *Transport in Porous Media* 77:267–285.
- Hossain, M. A., & Takhar, H. S. (1996). Radiation effect on mixed convection along a vertical plate with uniform surface temperature. *Heat Mass Transfer* 31:243-248.
- Ishak, A., Nazar, R., & Pop, I. (2006a). Unsteady mixed convection boundary layer flow due to a stretching vertical surface. *Arabian Journal for Science and Engineering* 31:165-182.
- Ishak, A., Nazar, R., & Pop, I. (2006b). Unsteady mixed convection boundary layer flow due to a stretching vertical surface. *The Arabian Journal for Science and Engineering* 31: 165 – 181.
- Ishak, A., Nazar, R., & Pop, I. (2007). Boundary layer flow of a micropolar fluid on a continuously moving or fixed permeable surface. *International Journal of Heat and Mass Transfer* 50:4743-4748.
- Ishak, A., Nazar, R., Pop, I. (2008a). Post-stagnation point boundary layer flow and mixed convection heat transfer over a vertical, linearly stretching sheet. *Archives of Mechanics* 60 (4): 303-322.
- Ishak, A., Nazar, R., Pop, I. (2008b). Mixed convection stagnation point flow of a micropolar fluid towards a stretching sheet. *Meccanica* 43:411-418.
- Ishak, A., Nazar, R., Pop, I. (2008c). Hydromagnetic flow and heat transfer adjacent to a stretching vertical sheet. *Journal of Heat Mass Transfer* 44: 921-927.

- Ishak, A., Nazar, R., Arifin, N. M., & Pop, I. (2008d). Dual solutions in mixed convection flow near a stagnation point on a vertical porous plate. *International Journal of Thermal Sciences* 47:417-422.
- Ishak, A. (2009). Radiation effects on the flow and heat transfer over a moving plate in a parallel stream. *Chinese Physics Letters* 26: 034701.
- Ishak, A., Nazar, R., Pop, I. (2009a). Boundary layer flow and heat transfer over an unsteady stretching vertical surface. *Meccanica* 44: 369-375.
- Ishak, A., Jafar, K., Nazar, R., & Pop, I. (2009b). MHD stagnation point flow towards a stretching sheet. *Physica A: Statistical Mechanics and its Applications* 388:3377-3383.
- Ishak, A., Lok, Y. Y., & Pop, I. (2010a). Stagnation-point flow over a shrinking sheet in a micropolar fluid. *Chemical Engineering Communications* 197: 1417–1427.
- Ishak, A., Nazar, R., Bachok, N., & Pop, I. (2010b). MHD mixed convection flow adjacent to a vertical plate with prescribed surface temperature. *International Journal of Heat and Mass Transfer* 53:4506-4510.
- Ishak, A. (2011). MHD boundary layer flow due to an exponentially stretching sheet with radiation effect. *Sains Malaysiana* 40:391-395.
- Karwe, M. V., & Jaluria, Y. (1988). Fluid flow and mixed convection transport from a moving plate in rolling and extrusion processes. *ASME Journal of Heat Mass Transfer* 110:655-661.
- Karwe, M. V., & Jaluria, Y. (1991). Numerical simulation of thermal transport associated with a continuously moving flat sheet in materials processing. *ASME Journal of Heat Transfer* 113:612-619.

- Keller, H. B. (1970). A new difference scheme for parabolic problems, in: J. Bramble 341 (Ed.), *Numerical Solution of Partial-Differential Equations*, vol. II. Academic, New York.
- Keller, H. B. & Cebeci, T. (1971). Accurate numerical methods for boundary layer flows, I: Two-dimensional laminar flow. *Proceeding of the 2nd International Conference on Numerical solutions of partial differential equations*. New York: Springer-Verlag.
- Keller, H. B. & Cebeci, T. (1972). Accurate numerical methods for boundary layer flows, II: Two-dimensional turbulent flows. *AIAA Journal* 10: 1193-1199.
- Kestin, J. (1966). *A course in Thermodynamics*. Vol. II, Blaisdell.
- Magyari, E. & Keller, B. (1999). Heat and mass transfer in the boundary layers on an exponentially stretching continuous surface. *Journal of Physics D: Applied Physics* 32: 577–585.
- Mahapatra, T. R., Nandy, S. K., Vajravelu, K., & Van Gorder, R. A. (2011). Stability analysis of fluid flow over a nonlinearly stretching sheet. *Archive Applied Mechanics* 81:1087-1091.
- Merkin, J. H., & Mahmood, T. (1989). Mixed convection boundary layer similarity solutions: prescribed wall heat flux. *Journal of Applied Mathematics and Physics* 40:51–68.
- Merkin, J. H., & Kumaran, V. (2010). The unsteady MHD boundary layer flow on a shrinking sheet. *European Journal of Mechanics B/Fluids* 29:357-363.
- Merkin, J. H. (1985). On dual solutions occurring in mixed convection in a porous medium. *Journal of Engineering Mathematics* 20:171–179.
- Miklavčič, M. & Wang, C. Y. (2006). Viscous flow due to a shrinking sheet. *Quarterly of Applied Mathematics* 64:283–290.

- Nadeem, S., & Awais, M. (2008). Thin film flow of an unsteady shrinking sheet through porous medium with variable viscosity. *Physics Letters A* 372:4965-4972.
- Nadeem, S., Abbasbandy, S., & Hussain, M. (2009). Series solutions of boundary layer flow of a micropolar fluid near the stagnation point towards a shrinking sheet. *Zeitschrift fur Naturforschung A* 64:575- 582.
- Nadeem, S., Hussain, A., & Vajravelu, K. (2010a). Effects of heat transfer on the stagnation flow of a third-order fluid over a shrinking sheet. *Zeitschrift fur Naturforschung A* 65:969-994.
- Nadeem, S., Hussain, A., & Khan, M. (2010b). Stagnation flow of a Jeffrey fluid over a shrinking sheet. *Zeitschrift fur Naturforschung A* 65:540-548.
- Nazar, R., Amin, N., Flip, D., & Pop, I. (2004). Unsteady boundary layer flow in the region of the stagnation point on a stretching sheet. *International Journal of Engineering Science* 42:1241-1253.
- Noor, N. F. M., Kechil, S. A., & Hashim, I. (2010). Simple non-perturbative solution for MHD viscous flow due to a shrinking sheet. *Communications in Nonlinear Science and Numerical Simulation* 15:144-148.
- Pal, D. (2010). Mixed convection heat transfer in the boundary layers on an exponentially stretching surface with magnetic field. *Applied Mathematics and Computation* 217:2356-2369.
- Postelnicu, A., & Pop, I. (2011). Falkner-Skan boundary layer flow of a power-law fluid past a stretching wedge. *Applied Mathematics and Computation* 217:4359–4368.
- Ramachandran, N., Chen, T. S., & Armaly, B. F. (1988). Mixed convection in stagnation flows adjacent to vertical surfaces. *ASME Journal of Heat Mass Transfer* 110: 373–377.

- Ridha, A. (1996). Aiding flows non-unique similarity solutions of mixed convection boundary layer equations. *Journal of Applied Mathematics and Physics (ZAMP)* 47:341-352.
- Saha, L. K., Hossain, M. A., & Gorla, R. S. R. (2007). Effect of Hall current on the MHD laminar natural convection flow from a vertical permeable flat plate with uniform surface temperature. *International Journal of Thermal Sciences* 46: 790–801.
- Sajid, M. & Hayat, T. (2008). Influence of thermal radiation on the boundary layer flow due to an exponentially stretching sheet. *International Communications in Heat and Mass Transfer* 35: 347–356.
- Sajid, M., Javed, T., & Hayat, T. (2008). MHD rotating flow of a viscous fluid over a shrinking surface. *Nonlinear Dynamics* 51:259-265.
- Sanjayanand, E. & Khan, S. K. (2006). On heat and mass transfer in a viscoelastic boundary layer flow over an exponentially stretching sheet. *International Journal of Thermal Sciences* 45:819-828.
- Schlichting, H. (1979). *Boundary-Layer Theory*, 7th ed. New York: McGraw-Hill.
- Van Gorder, R. A. (2010). High-order nonlinear boundary value problems admitting multiple exact solutions with application to the fluid flow over a sheet. *Applied Mathematics and Computation* 216:2177-2182.
- Van Gorder, R. A., & Vajravelu, K. (2011). Multiple solutions for hydromagnetic flow of a second grade fluid over a stretching or shrinking sheet. *Quarterly of Applied Mathematics* 69:405-424.
- Wang, C. Y. (2008). Stagnation flow towards a shrinking sheet. *International Journal of Non-linear Mechanics* 43: 377–382.

- Weidman, P. D., Kubitschek, D. G., & Davis, A. M. J. (2006). The effect of transpiration on self-similar boundary layer flow over moving surface. *International Journal of Engineering Science* 44:730–737.
- Weidman, P. D., & Ali, M. E. (2011). Aligned and nonaligned radial stagnation flow on a stretching cylinder. *European Journal of Mechanics B/Fluids* 30:120-128.
- White, F. M. (2000) *Viscous Fluid Flow*, 3rd ed. New York: McGraw-Hill.
- Yih, K. A. (1998). Coupled heat and mass transfer in mixed convection over a vertical flat plate embedded in saturated porous media: PST/PSC or PHF/PMF. *Heat and Mass Transfer* 34: 55-61.